AD_____

Award Number: W81XWH-08-1-0414

TITLE: Identification and Targeting of Upstream Tyrosine Kinases Mediating PI3 Kinase Activation in PTEN Deficient Prostate Cancer

PRINCIPAL INVESTIGATOR: Steven P. Balk

CONTRACTING ORGANIZATION: Beth Israel Deaconess Medical Center
Boston, MA 02215

REPORT DATE: June 2011

TYPE OF REPORT: Final

PREPARED FOR: U.S. Army Medical Research and Materiel Command
Fort Detrick, Maryland 21702-5012

REPORT DOCUMENTATION PAGE

Form Approved
OMB No. 0704-0188

1. REPORT DATE	2. REPORT TYPE	3. DATES COVERED
June 2011	Final	1 June 2008 – 31 May 2011

4. TITLE AND SUBTITLE

Identification and Targeting of Upstream Tyrosine Kinases Mediating PI3 Kinase Activation in PTEN Deficient Prostate Cancer

5a. CONTRACT NUMBER

5b. GRANT NUMBER
W81XWH-08-1-0414

5c. PROGRAM ELEMENT NUMBER

6. AUTHOR(S)

Steven P. Balk

E-Mail: sbalk@bidmc.harvard.edu

5d. PROJECT NUMBER

5e. TASK NUMBER

5f. WORK UNIT NUMBER

7. PERFORMING ORGANIZATION NAME(S) AND ADDRESS(ES)

Beth Israel Deaconess Medical Center
Boston, MA 02215

8. PERFORMING ORGANIZATION REPORT NUMBER

9. SPONSORING / MONITORING AGENCY NAME(S) AND ADDRESS(ES)
U.S. Army Medical Research and Materiel Command
Fort Detrick, Maryland 21702-5012

10. SPONSOR/MONITOR'S ACRONYM(S)

11. SPONSOR/MONITOR'S REPORT NUMBER(S)

12. DISTRIBUTION / AVAILABILITY STATEMENT
Approved for Public Release; Distribution Unlimited

13. SUPPLEMENTARY NOTES

14. ABSTRACT

The PI3K pathway is activated by PTEN loss in most prostate cancers (PCa), but the contribution of upstream RTKs that may be targeted therapeutically has not been assessed. Immunoblotting of p85 associated proteins in PTEN deficient LNCaP and C4-2 PCa cells showed a small set of tyrosine phosphorylated proteins, but they were not recognized by an anti-pYxxM motif antibody and were not found in PTEN deficient PC3 PCa cells. LC/MS/MS and immunoblotting showed that p85 was associated primarily with p110 and p110 . Basal tyrosine phosphorylation of p110 and p110 could be blocked by c-Src inhibitors, but this did not suppress PI3K activity, which was similarly independent of Ras. Basal PI3K activity was mediated by p110 in PC3 cells, and by both p110 and p110 in LNCaP cells, while p110 was required for PI3K activation in response to RTK stimulation by heregulin- 1. These findings show that basal PI3K activity in PTEN deficient PCa cells is RTK independent and can be mediated by p110 and p110 . Increased p110 expression in PCa may be required for RTK independent PI3K pathway activation in adult prostate epithelium with genetic or epigenetic PTEN downregulation.

15. SUBJECT TERMS
prostate cancer, PI3 kinase, receptor tyrosine kinase

16. SECURITY CLASSIFICATION OF:			17. LIMITATION OF ABSTRACT	18. NUMBER OF PAGES	19a. NAME OF RESPONSIBLE PERSON
a. REPORT	b. ABSTRACT	c. THIS PAGE			USAMRMC
U	U	U	UU	35	19b. TELEPHONE NUMBER *(include area code)*

Table of Contents

INTRODUCTION

PI3 kinase pathway activation is common in advanced prostate cancer (PCa) and is mediated primarily by PTEN loss, suggesting that it may be independent of activation by upstream receptor tyrosine kinases (RTKs) or nonreceptor tyrosine kinases and therefore unresponsive to tyrosine kinase inhibitors. However, in studies presented in the proposal, we found that the p85 regulatory subunit of PI3 kinase is associated constitutively with ErbB3 and two other tyrosine phosphorylated proteins in PTEN deficient LNCaP and C4-2 PCa cells. Treatment with an ErbB2 inhibitor (lapatinib) did not rapidly decrease PI3 kinase activity, but combined treatment with lapatinib and sorafenib (a multi-kinase inhibitor) was as effective as a direct PI3 kinase antagonist (LY294002) at blocking PI3 kinase activity. Based on these data, we hypothesized that a small number of upstream RTKs (or nonreceptor tyrosine kinases) may be critical for PI3 kinase activation in PTEN deficient PCa, and that targeting these tyrosine kinases may be an effective approach for suppressing PI3 kinase activity and PCa growth *in vivo*. The objective of this proposal was to test these hypotheses, and more generally determine the molecular basis for basal PI3 kinase activity in PTEN deficient PCa cells. The specific aims were as follows:

Aim 1. Identify the p85 associated tyrosine phosphorylated proteins in PTEN deficient LNCaP and C4-2 PCa cells lines, and determine whether they mediate PI3 kinase activation.

Aim 2. Test the hypothesis that receptor tyrosine kinase inhibitors can be used to block p85 membrane recruitment and suppress PI3 kinase activity *in vivo* in PCa xenografts.

BODY

Aim 1. Identify the p85 associated tyrosine phosphorylated proteins in PTEN deficient LNCaP and C4-2 PCa cells lines, and determine whether they mediate PI3 kinase activation. In our initial preliminary studies we had found that a series of tyrosine phosphorylated proteins were associated with p85 in LNCaP and C4-2 cells, and also showed that p85 was associated with ErbB3. Therefore, we first focused on whether ErbB3 was one of the detected p85 associated tyrosine phosphorylated proteins, and its role in PI3 kinase activation.

p85 interaction with ErbB3 is independent of ErbB3 phosphorylation and ErbB2 activity. We found previously that p85 was associated with ErbB3 (Fig. 1A), but it was not clear if ErbB3 was one of the major tyrosine phosphorylated proteins associated with p85 or whether it was mediating or contributing to PI3 kinase activation. Therefore, we further examined whether the p85 interaction with ErbB3 was dependent on ErbB3 phosphorylation and mediating PI3 kinase activation**.** To test this hypothesis, we determined whether initially depleting ErbB3 by immunoprecipitation with anti-ErbB3 would decrease the p85 associated ~190 kDa tyrosine phosphorylated band in a subsequent anti-p85 immunoprecipitation. As shown in figure 1B, ErbB3 could be substantially depleted from the lysate by an initial immunoprecipitation with anti-ErbB3. The ErbB-3 depletion also markedly decreased the amount of ErbB3 that was coprecipitated with p85. However, this ErbB-3 depletion did not decrease the intensity of the tyrosine phosphorylated band at ~190 kDa or other bands that were coprecipitated by anti-p85. Moreover, the pTyr blot further indicated that ErbB3 immunoprecipitated by the anti-ErbB3 Ab was not substantially tyrosine phosphorylated.

This result indicated that ErbB3 was not one of the major the tyrosine phosphorylated proteins associated with p85. However, we could not rule out the possibility that a small pool of heavily tyrosine phosphorylated ErbB3 was associated with p85, and was not cleared by the anti-ErbB3. Therefore, we next used siRNA to downregulate ErbB3 expression. As shown in figure 1C, total ErbB3 expression was markedly reduced by ErbB3 siRNA versus a control siRNA. Moreover, p85 associated ErbB3 was also decreased, although it again appeared that this decrease was less marked than the decrease in total ErbB3. Importantly, there was again no decrease in the p85 associated tyrosine phosphorylated protein at ~190 kDa (Fig. 1D). Moreover, there was no evident effect of the ErbB3 siRNA on PI3 kinase activity, as assessed by Akt phosphorylation at S473 or T308 (Fig. 1C).

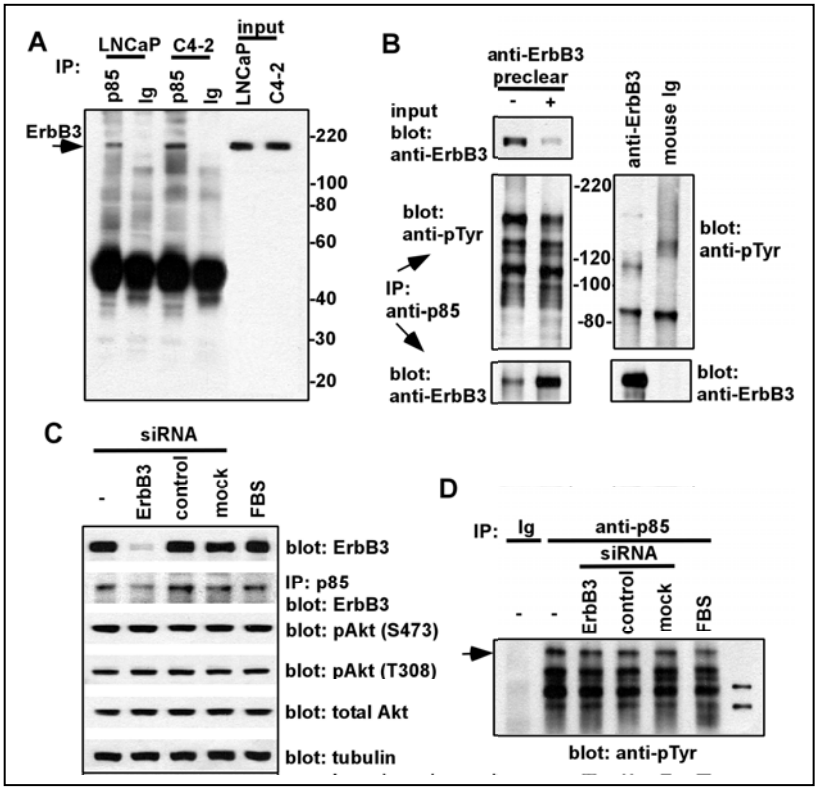

Figure 1. p85 interaction with ErbB-3 is not dependent on tyrosine phosphorylation in LNCaP cells. A, Lysates from serum starved LNCaP or C4-2 cells (2 days) were precipitated with anti-p85 (p85) or control rabbit IgG (Rab IgG), followed by blotting for ErbB-3. Input is 1% of the material used for the precipitation. B, LNCaP cells maintained in medium with 10% FBS were lysed in TBS buffer with 1% TX-100 and immunoprecipitated with anti-ErbB-3 and anti-p85 sequentially or with normal mouse serum (NMS) as control. The immunoprecipitates were immunoblotted with anti-p-Tyr or anti-ErbB-3. C and D, LNCaP cells transfected with siRNA of ErbB-3 or non-targeted control siRNA were maintained in RPMI-1640 with 10% FBS for 24 hr followed by serum starvation for 48 hr. Cell lysates were immunoprecipitated with anti-p85 followed by immunoblotting for anti-ErbB-3 (C) or anti-p-Tyr (D). Meanwhile, whole cell lysates (10μg) were subjected to immunoblotting for anti-pAkt to assess the PI3 kinase activity (C). Molecular markers are indicated at the margins.

Taken together, these results demonstrated that p85 was constitutively associated with ErbB3 in LNCaP cells, but indicated that ErbB3 was not one of the major tyrosine phosphorylated proteins associated with p85. To further address whether ErbB3 phosphorylation made any contribution to the p85-ErbB3 interaction, we treated LNCaP cells with a dual EGFR/ErbB2 inhibitor (lapatinib) to suppress any basal tyrosine phosphorylation of ErbB3. Using an anti-pTyr immunoprecipitation followed by immunoblotting to detect tyrosine phosphorylated proteins, we found that lapatinib suppressed the basal tyrosine phosphorylation of both EGFR and ErbB2 (Fig. 2A). In contrast, there was no detectable tyrosine phosphorylation of ErbB3 in the presence or absence of lapatinib (10μM for 6 hours), and no effect of lapatinib on Akt phosphorylation. Moreover, lapatinib did not decrease the interaction between p85 and ErbB3, strongly supporting the conclusion that this interaction is independent of ErbB3 phosphorylation (Fig. 2B).

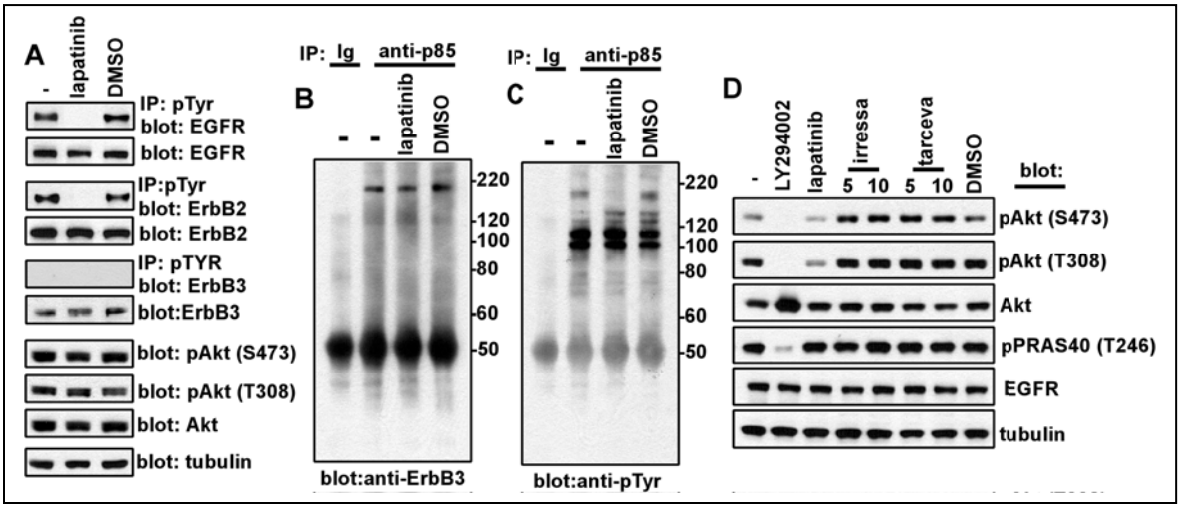

Figure 2. ErbB-2 inhibition suppresses PI3 kinase activity in LNCaP cells independently of tyrosine phosphorylation of ErbB-3. A-C, serum starved LNCaP cells (2 days) were treated with EGFR/ErbB-2 dual inhibitor lapatinib or vehicle (DMSO) for 6 hr at the concentration of 10μM. A, cell lysates were immunoprecipitated with anti-p-Tyr followed by immunoblotting for anti-EGFR, ErbB-2, or ErbB-3. Phosphorylation of Akt was also assessed. B and C, cell lysates were immunoprecipitated with anti-p85 or rabbit IgG followed by immunoblotting for anti-ErbB-3 (B) or anti-p-Tyr (C). D, serum starved LNCaP cells (2 days) were treated with PI3 kinase inhibitor LY294002 (20μM) for 2 hr, lapatinib (5μM) for 24 hr, EGFR inhibitors Iressa (5 or 10μM) or Tarceva (5 or 10μM) for 24 hr. Cell lysates (10μg) were subjected to immunoblotting analysis for PI3 kinase activity. Molecular markers are indicated at the margins for panels B and C.

Surprisingly, the intensity of the p85 associated band at ~190 kDa detected by pTyr immunoblotting was selectively decreased by lapatinib, suggesting that it may be an EGFR or ErbB2 substrate (Fig. 2C). Based on this observation, we further examined the effects of longer exposure to lapatinib on PI3 kinase activity. After 24 hours, lapatinib at 5 μM decreased Akt phosphoryation, although phosphorylation of an Akt substrate (PRAS40) was not effected (Fig. 2D). In contrast to these effects of lapatinib, Akt phosphorylation was not decreased by two EGFR specific inhibitors (Irressa and Tarceva), indicating that the effects of lapatinib were mediated through inhibition of ErbB2.

P85 association with tyrosine phosphorylated proteins is not mediated by direct p85 SH2 domain binding. The p85 subunits associate with tyrosine phosphorylated proteins primarily through their SH2 domains, which bind to proteins bearing pYxxM motifs. To determine whether constitutive tyrosine phosphorylation of a specific protein was mediating p85 recruitment directly through SH2 domain binding, we next immunoblotted the p85 immunoprecipitates with a pYxxM motif specific antibody. This antibody weakly detected several discrete p85 associated proteins between 130-200 kDa in lysates from LNCaP cells grown in 10% FBS (Fig. 3B). Discrete major p85 associated bands at ~190 kDa were detected by the anti-pYxxM antibody after EGF or heregulin-β1 stimulation, with the band after heregulin-β1 being consistent with ErbB3 (which contains 6 pYxxM motifs). In contrast, the pYxxM antibody did not detect discrete p85 associated proteins, or proteins corresponding to those found by pTyr blotting, in lysates from cells cultured in serum free medium (Fig. 3B). As a further sensitive assay to determine whether proteins containing pYxxM motifs were present in serum starved LNCaP cells, whole cell lysates were immunoprecipitated with an anti-pTyr Ab and then immunoblotted with the pYxxM motif Ab. As shown in figure 3C, several bands could be detected when cells were grown in 10% FBS or were stimulated with EGF or heregulin-β1, but not in the serum starved cells. Taken together, these data indicated that the association between p85 and tyrosine phosphorylated proteins was not mediated by direct p85 SH2 domain binding.

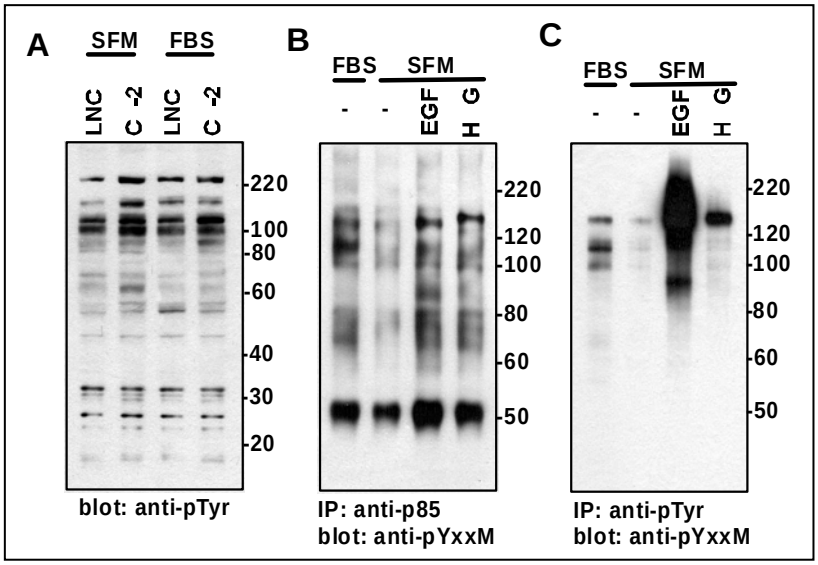

Figure 3. p85 association with tyrosine phosphorylated proteins in serum starved PTEN deficient cells LNCaP cells is not mediated by the p85 SH2 domain. A, cell lysates (10 g) from LNCaP or C4-2 cells grown in serum free medium (SFM) as well as in medium with 10% FBS were immunoblotted for anti-p-Tyr to assess tyrosine phosphorylated proteins. B and C, LNCaP cells were either maintained in medium with 10%FBS or serum starved for 2 days. Serum starved cells were then stimulated with EGF (20ng/ml, 5 min) or HRG-β1 (40ng/ml, 15 min). Cell lysates were immunoprecipitated with anti-p85 (B) or anti-p-Tyr (C) and the immunoprecipitates were blotted with anti-pYXXM. Molecular markers are indicated at the margins.

PI3K is not associated with tyrosine phosphorylated proteins in PC3 cells. The data above in conjunction with our previous data indicated that ErbB2, in conjunction with one or more

kinases targeted by sorafenib, contributed to PI3K pathway activation in PTEN deficient LNCaP cells. Moreover, this inhibition correlated with loss of tyrosine phosphorylated p85 associated proteins. However, we could not conclude from these results whether these tyrosine phosphorylated proteins were required for p85 membrane recruitment and PI3K activation. Therefore, to further assess the possible importance of p85 membrane recruitment by tyrosine phosphorylated proteins, we examined p85 associated proteins from PC3 cells (also a PTEN deficient PCa cell line) and a series of other cell lines. Significantly, the only tyrosine phosphorylated band associated with p85 in PC3 cells was ~110 kDa, consistent with the p110 catalytic subunit of PI3K (Fig. 4A). This band was also found in a subset of other cell lines, with no other tyrosine phosphorylated bands being common to multiple cells.

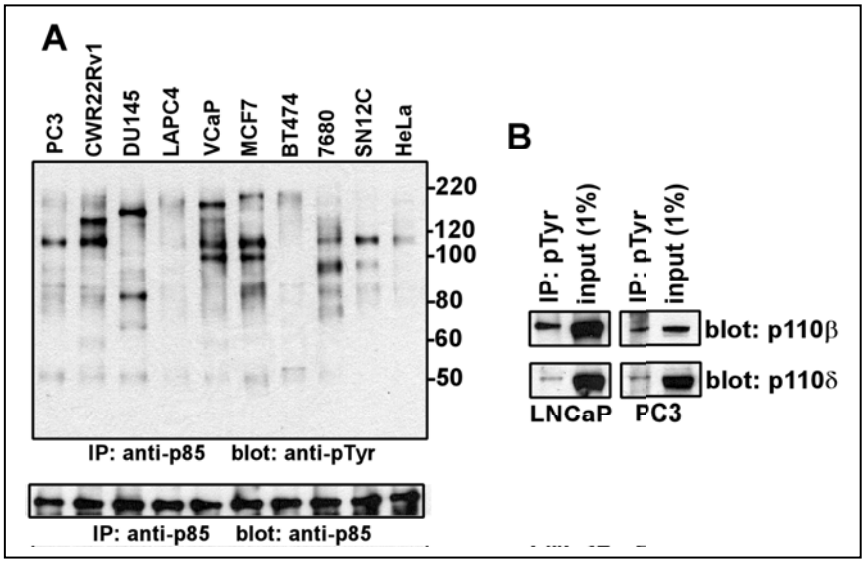

Figure 4. p85 is not associated with multiple tyrosine phosphorylated proteins in PC-3 cells. A, human prostate cancer cell lines PC-3, 22Rv1, Du145, LAPC4, VCaP, human breast cancer lines MCF-7, BT474, human renal carcinoma cell lines 786O (PTEN deficient), SN12C, and human cervix caner cell line Hela were serum starved for 1 day. Cell lysates were immunoprecipitated with anti-p85 and the immunoprecipitates were immunoblotted for anti-p-Tyr or anti-p85. Molecular markers are indicated at the left margin. B, Serum starved LNCaP (2 days) and PC-3 cells (1 day) were lysed and immunoprecipitated with anti-p-Tyr followed by immunoblotting for anti-p110β or δ. Input is 1% of the material used for the precipitation.

To support the conclusion that the tyrosine phosphorylated protein at ~110 kDa was the PI3K catalytic subunit, we carried out anti-pTyr immunoprecipitations followed by immunoblotting for each of the p110 isoforms. As shown in figure 4B, total p110β levels were higher in LNCaP versus PC3 cells (inputs), but comparable levels were precipitated by the anti-pTyr antibody (with this blot indicating that ~1% of p110β in serum starved PC3 cells is tyrosine phosphorylated). It should be noted that p110 in these experiments may be precipitated indirectly through an association with another tyrosine phosphorylated protein such as p85 in LNCaP cells, although the p110 precipitation from PC3 is more likely direct as there is no detectable tyrosine phosphorylation of p85 in these cells (Fig. 4A). In contrast to p110β, expression of p110δ is more comparable in LNCaP and PC3 cells, and only a very small fraction appears to be tyrosine

phosphorylated. Finally, there was no detectable tyrosine phosphorylation of p110α in either cell (data not shown).

ErbB2 inhibition suppresses PI3K activity in PC3 cells. The above results indicated that basal PI3K activity in PC3 cells was not dependent on p85 recruitment by an activated RTK or tyrosine phosphorylated adaptor protein. Therefore, we next determined whether basal PI3K activity in serum starved PC3 cells was still inhibited by lapatinib or sorafenib. In contrast to LNCaP cells, lapatinib at 5-10 μM was able to rapidly suppress PI3K activity in serum starved PC3 cells (Fig. 5A) and in PC3 cells grown in 10% FBS (Fig. 5B). Sorafenib by itself was not clearly active, but could enhance the activity of lapatinib, supporting the conclusion that these drugs were inhibiting PI3K pathway activity by a mechanism distinct from preventing SH2 domain mediated recruitment of p85. As in LNCaP cells, the EGFR specific inhibitors (Irressa and Tarceva) were much less effective than lapatinib, indicating that the effects of lapatinib were due to ErbB2 inhibition (Fig. 5C). Consistent with this conclusion, EGFR downregulation by shRNA had no apparent effect on Akt phosphorylation or activity (as assessed by PRAS40 phosphorylation) in the PC3 cells (Fig. 5D).

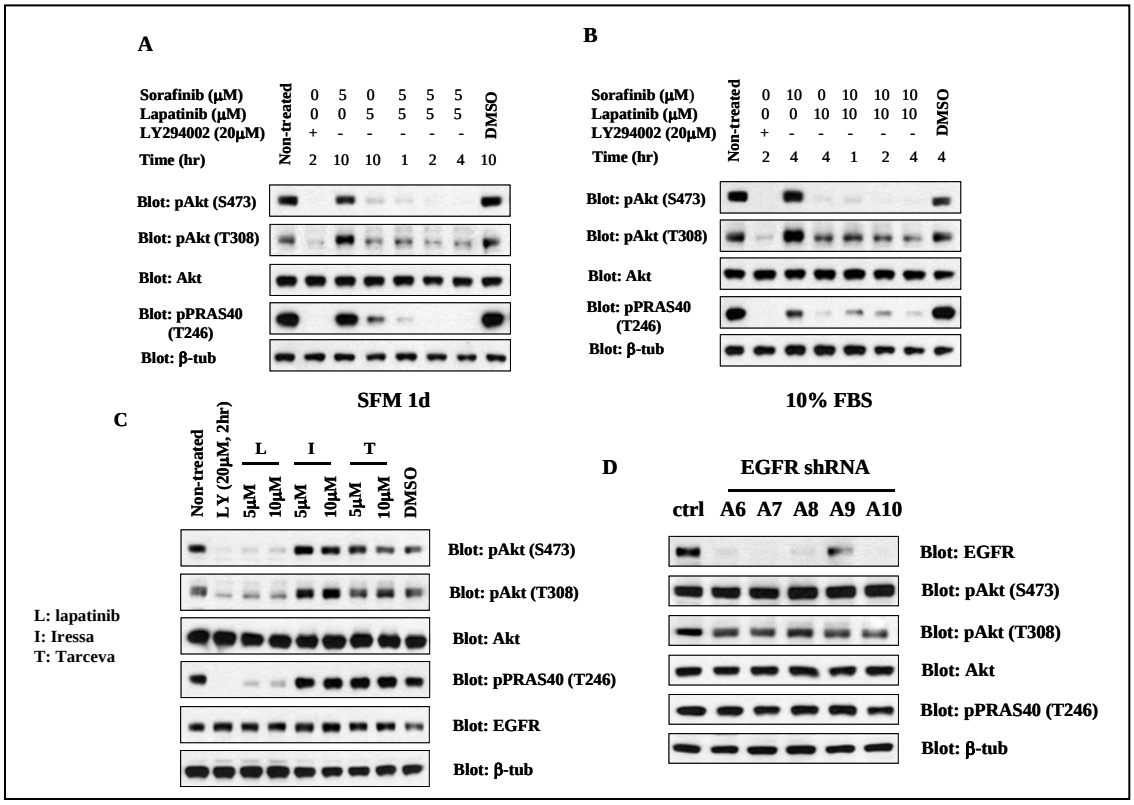

Figure 5. ErbB2 inhibition strongly suppresses PI3 kinase activity in PC-3 cells. A, PC-3 cells were serum starved for 1 day and then treated with sorafenib (5μM, 10 hr), lapatinib (5μM, 10 hr), or combination (5μM each) for 1, 2, or 4 hours. Whole cell lysates (10μg) were immnolotted with anti-pAkt or anti-pPRAS40 to assess PI3 kinase activity, B, PC-3 cells grown in medium with 10% FBS were treated with sorafenib (10μM, 4 hr), lapatinib (10μM, 4 hr), or combination (10μM each) for 1, 2 , or 4 hours, and cell lysates (10μg) were immnolotted for anti-pAkt or anti-pPRAS40. C, serum starved PC-3 cells (1 day) were treated with PI3 kinase inhibitor LY294002 (20μM) for 2 hr, lapatinib (5 or 10μM) for 24 hr, EGFR inhibitors Iressa (5

or 10μM) or Tarceva (5 or 10μM) for 24 hr. Cell lysates (10μg) were immnolotted with anti-pAkt or anti-pPRAS40. D, PC-3 cells were infected with virus containing EGFR shRNAs (A6, A7, A8, A9 or A10). Cells were maintained in DMEM medium with 10% FBS for 2 days and then serum starved for 1 day. Cell lysates (10μg) were immnolotted with anti-pAkt or anti-pPRAS40.

p110 tyrosine phosphoryation is mediated by c-Src and does not regulate PI3K activity. Although the functional significance of p110 tyrosine phosphorylation is not clear, based on these results we considered that lapatinib or sorafenib may be suppressing p110 catalytic activity by inhibiting its tyrosine phosphorylation. However, p85 immunoprecipitations followed by pTyr immunoblotting showed that neither lapatinib or sorafenib treatment, or the combination, decreased tyrosine phosphoryation of the p85 associated p110 band in PC3 cells (Fig. 6A). Similarly, pTyr immunoprecipitations followed by p110 immunoblotting indicated that p110β and p110δ tyrosine phosphorylation were not affected by lapatinib or sorafenib, or by the combination (Fig. 6B). Importantly, blotting for pAkt and pPRAS40 indicated that PI3K activity was decreased within 2 hours by the combined lapatinib plus sorafenib used in this experiment (Fig. 6B).

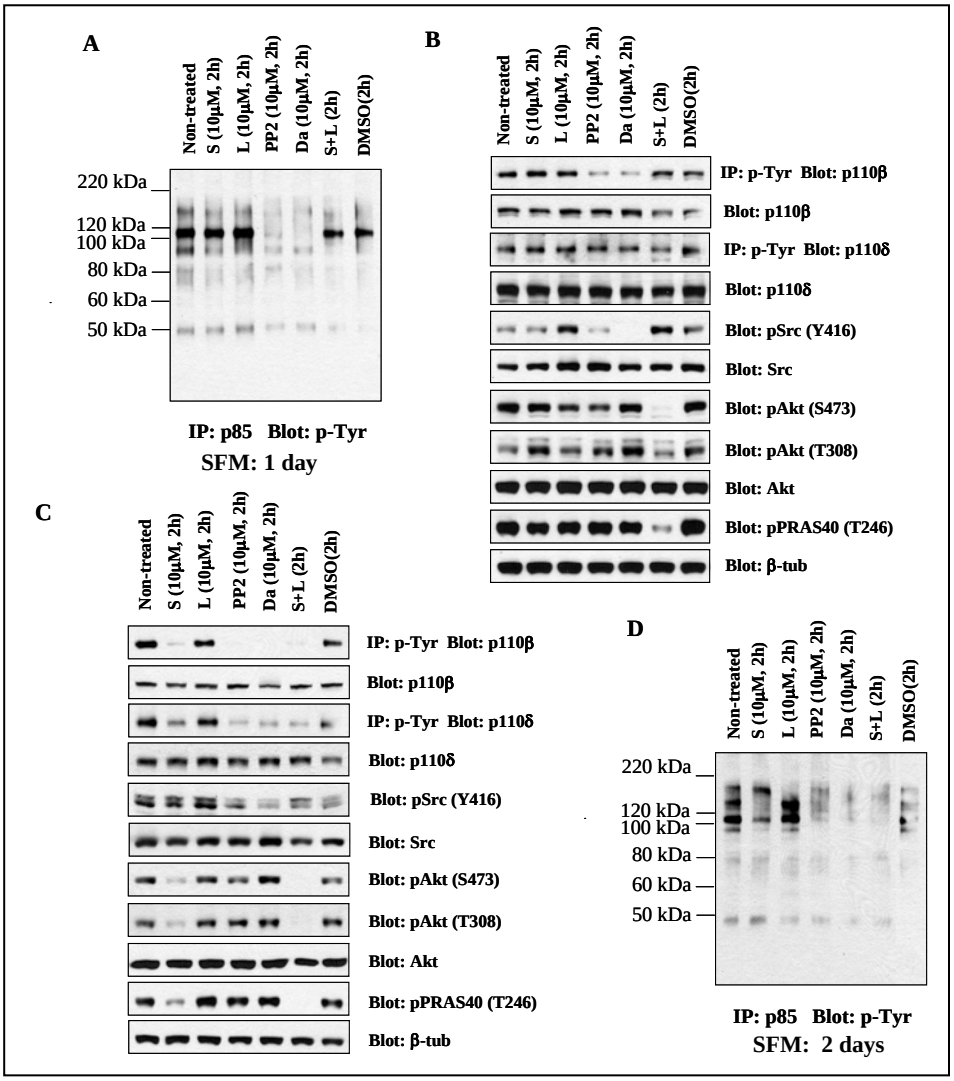

Figure 6. Phosphorylation of p110β and p110δ are mediated by c-Src but not correlated with PI3 kinase activity. A and B, serum starved PC-3 cells (1 day) were treated with sorafenib, lapatinib, combined sorafenib and lapatinib, Src inhibitors PP2 or dasatinib for 2 hr, all at 10μM. A, cell lysates (10μg) were immunoprecipitated with anti-p85 and the immunoprecipitates were immunoblotted for anti-p-Tyr. B, cell lysates were immunoprecipitated with anti-p-Tyr followed by immunoblotting for anti-p110β or δ. Whole cell lysates (10μg) were immunoblotted with pSrc, pAkt, pPRAS40, total Src or Akt. C and D, serum starved LNCaP cells (2 days) were treated with sorafenib, lapatinib, combined sorafenib and lapatinib, PP2 or dasatinib for 2 hr, all at 10μM. B, cell lysates were immunoprecipitated with anti-p-Tyr followed by blotting for anti-p110β or δ. Whole cell lysates (10μg) were immunoblotted with pSrc, pAkt, pPRAS40, total Src or Akt. D, cell lysates were immunoprecipitated with anti-p85 and the immunoprecipitates were immunoblotted with anti-p-Tyr. Molecular markers are indicated at the left margins of panels A and D.

We next examined the Phosphosite and Scansite databases to determine previously identified sites of tyrosine phosphorylation on the PI3 kinase p110 catalytic subunits and candidate kinases for these sites, which suggested phosphorylation by c-Src family kinases. Strikingly, treatment with c-Src inhibitors (PP2 or dasatinib) resulted in the rapid and complete loss of p110 tyrosine phopshorylation in serum starved PC3 cells, as shown by p85 immunoprecipitation followed by pTyr blotting (Fig. 6A). Consistent with p110β being the predominant tyrosine phosphorylated p110 isoform in PC3 cells (see Fig. 5B), pTyr immunoprecipitation followed by p110 blotting showed a marked decline in p110β tyrosine phosphorylation (Fig. 6B). However, in contrast to the effects of sorafenib plus lapatinib, c-Src inhibition did not markedly suppress Akt phosphorylation or activity. It should again be noted that p110 may be precipitated by anti-pTyr through an association with another tyrosine phosphorylated protein. However, the coincident loss of the p85 associated tyrosine phosphorylated band at 110 (Fig. 6A) indicates that c-Src inhibitors are directly decreasing p110β and p110δ phosphorylation.

PP2 and dasatinib also markedly decreased both p110β and p110δ tyrosine phosphorylation in LNCaP cells, but again did not significantly decrease Akt phosphorylation or activity (Fig. 6C). Moreover, the tyrosine phosphoryated p85 associated bands at ~130-190 kDa in LNCaP cells were also markedly diminished by c-Src inhibition (Fig. 6D). The loss of these latter bands, without an effect of PI3K pathway activity, further supports the conclusion that PI3K activity is not dependent on p85 recruitment by a tyrosine phosphorylated RTK or adaptor protein.

p85 associated proteins identified by LC/MS/MS. An alternative approach we next took to identify p85 associated proteins was liquid chromatography/tandem mass spectrometry (LC/MS/MS). Anti-p85 beads were used to carry out large scale immunopurifications from serum starved LNCaP cells, which were then run on SDS-PAGE. Multiple gel slices corresponding to protein molecular weights from ~60-220 kDa were then subjected to in-gel trypsin digestion, and eluted peptides were identified by LC/MS/MS (Table 1) using a linear ion trap mass spectrometer. As expected, a large fraction of the peptides detected in the ~100 kDa range were from the α and β isoforms of p85 and the p110 PI3K catalytic subunits. Interestingly, peptide recovery indicated that p110β and p110δ were the major p85 associated p110 isoforms, with much lower levels of p110α. Amongst the p85 associated proteins identified initially by

LC/MS/MS, only ErbB3 had been shown previously to mediate p85 SH2 domain binding and PI3K activation (Table 1). On a subsequent LC/MS/MS analysis of the p85 immunoprecipitates using a more sensitive Orbitrap XL mass spectrometer, we also detected GAB1 (Table 1). However, we could not detect GAB1 associated with p85 by immunoblotting (data not shown). Consistent with the LC/MS/MS data, we similarly did not find detectable levels of ErbB2, EGFR, c-MET, IGFR, insulin receptor, IRS-2, or IRS-4 (LNCaP are IRS-1 deficient) in the p85 immunoprecipitates by immunoblotting (data not shown).

Table1. p85 associated proteins identified by LC/MS/MS in LNCaP cells

Accession	Protein Name	Spectral count
PIK3R2	Phosphatidylinositol 3-kinase regulatory subunit beta	34
PK3CB	Phosphatidylinositol-4,5-bisphosphate 3-kinase catalytic subunit beta isoform	25
PK3CD	Phosphatidylinositol-4,5-bisphosphate 3-kinase catalytic subunit delta isoform	24
PIK3R1	Phosphatidylinositol 3-kinase regulatory subunit alpha	17
MAP1B	Microtubule-associated protein 1B	12
EWS	RNA-binding protein EWS	10
FAS	Fatty acid synthase	8
MYH10	Myosin-10	8
LIMC1	LIM and calponin homology domains-containing protein 1	6
RFIP1	Rab11 family-interacting protein 1	6
MYH9	Myosin-9	5
MYO6	Myosin-VI	5
PK3CA	Phosphatidylinositol-4,5-bisphosphate 3-kinase catalytic subunit alpha isoform	5
TERA	Transitional endoplasmic reticulum ATPase	5
SYEP	Bifunctional aminoacyl-tRNA synthetase	4
IF4G1	Eukaryotic translation initiation factor 4 gamma 1	4
ILF3	Interleukin enhancer-binding factor 3	4
PNPT1	Polyribonucleotide nucleotidyltransferase 1, mitochondrial	4
SFPQ	Splicing factor, proline- and glutamine-rich	4
SMRC1	SWI/SNF complex subunit SMARCC1	4
DHX9	ATP-dependent RNA helicase A	3
RAD50	DNA repair protein RAD50	3
MATR3	Matrin-3	3
TPR	Nucleoprotein TPR	3
K1967	Deleted in breast cancer gene 1 protein (DBC.1) (DBC-1) (p30 DBC)	3
TFR1	Transferrin receptor protein 1	3
SC16A	Protein transport protein Sec16A	2
ERBB3	Receptor tyrosine-protein kinase erbB-3	2
GAB1[1]	GRB2-associated-binding protein 1	2
NUCL	Nucleolin	1

[1]identified in a subsequent analysis focused on targeting peptides from known p85 interacting proteins

PI3K pathway activity in PTEN deficient PCa cells is Ras independent. An alternative mechanism by which RTKs may recruit and activate PI3K is by generating GTP-Ras, which can bind to the p110 subunits via Ras binding domains located carboxy to the p85 binding domains. GTP-Ras has been shown to enhance p110α activity, and an intact p110α-Ras interaction is required for Ras mediated tumorgenesis, although the importance of GTP-Ras for other p110 isoforms has not been established. The LC/MS/MS analysis of p85 associated proteins from LNCaP cells did not reveal an association of Ras, and this was confirmed by immunoblotting of anti-p85 immunoprecipitates with a pan-anti-Ras antibody (data not shown). However, a weak

transient interaction could not be excluded. Therefore, to further assess whether Ras was contributing to PI3K pathway activation, we treated serum starved LNCaP and PC3 cells with a farnesylation inhibitor, FTI-277. Immunoblotting with a pan-anti-Ras Ab confirmed that the drug prevented formation of the more rapidly migrating farnesylated protein (fRas), but there was no effect on PI3K pathway activation in serum starved LNCaP or PC3 cells (Fig. 7). It should be noted that the drug did not abrogate EGF mediated Erk activation, indicating either that adequate Ras could still be recruited (farnesylated or independent of farnesylation) or that EGFR was signaling independently of Ras.

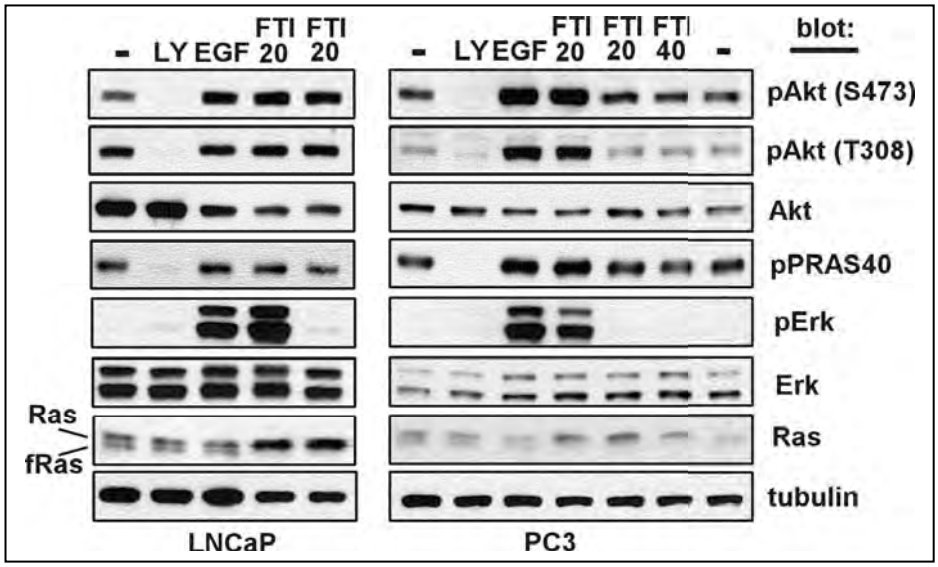

Figure 7. PI3K pathway activity in PTEN deficient PCa cells is Ras independent. LNCaP or PC3 cells plated into 24-well plates were treated with farnesylation inhibitor FTI-277 (20 or 40 μM; prepared in serum free medium) for 2 days, non-drug treated wells were serum starved for the same duration. At the end of FTI-277 treatment, cells were either treated with LY294002 (20 μM, 2 hr) or stimulated with EGF (20 ng/ml, 5 min). Whole cell lysates (10 μg) were analyzed by immunoblotting for pAkt, pPRAS40, total Akt, Erk1/2, pErk1/2, Ras, or tubulin. Upper and lower bands corresponding to Ras and farnesylated Ras (fRas) are indicated.

p110 isoforms associated with p85 in PCa cells. It was noteworthy that the LC/MS/MS analysis of p85 associated proteins in LNCaP cells indicated that p110β and p110δ were the major isoforms (Table 1). In addition, a label-free quantitative LC/MS/MS analysis based on the calculated average total ion current (TIC) of all identified peptides corresponding to PI3K protein subunits was utilized to quantify the relative abundance of PI3K regulatory and catalytic subunits in both LNCaP and PC3 cell lines. This analysis for LNCaP was consistent with Table 1, and for PC3 cells also showed lower levels of p110α, although the levels in PC3 were closer to those of p110β and p110δ (Fig. 8A and Tables 2 and 3 for PI3K quantification). Results from immunoblotting LNCaP and PC3 whole cell lysates with isoform specific p110 Abs were in general agreement with the LC/MS/MS data (Fig. 8B). Moreover, the immunoblotting indicated that p110α levels in LNCaP and PC3 cells were lower than in a small series of breast cancer lines and in PCa cells with intact PTEN (VCaP and CWR22) (Fig. 8B). Interestingly, available cDNA/oligonucleotide microarray data show that p110β and p110δ mRNA, but not p110α

mRNA, are increased in PCa versus normal prostate (Fig. 8C). In contrast, microarray data in GBM, which is also characterized by PTEN loss, shows that p110β is decreased (Fig. 8C).

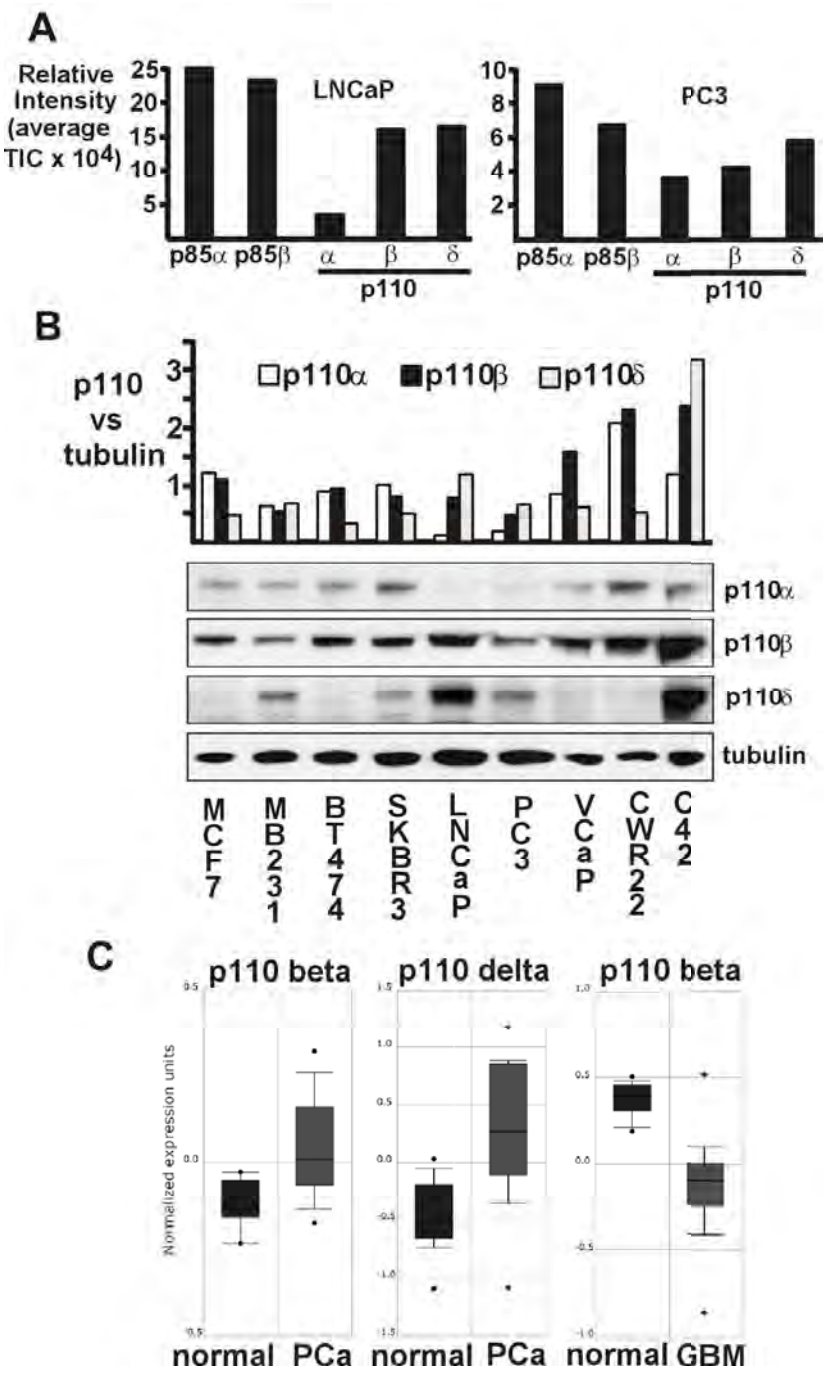

Figure 8. Expression of PI3K p110 isoforms in PCa cell lines. A, LC/MS/MS analyses of the relative abundance by average TIC of the PI3K subunits p85α, β and p110α, β, δ in LNCaP and PC3 cells. B, Expression levels of p110 isoforms in a variety of cancer cell lines based on immunoblotting. 10 μg of cell lysates from breast cancer lines (MCF-7, MB-MDA-231, BT-474, SKBR-3) or PCa cell lines (LNCaP, PC3, VCaP, CWR22Rv1, C4-2) were analyzed by immunoblotting with p110 isoform specific antibodies. Intensity of each band relative to tubulin is shown. C, p110β and p110δ mRNA levels in normal prostate versus PCa or normal brain versus GBM. Expression data generated by Oncomine based on results from Vanaja et al., (PCa p110β), Dhanasekaran et al., (PCa p110δ), and Sun et al. (GBM).

Distinct p110 isoforms mediate basal versus growth factor stimulated PI3K activity. Based on these observations, we addressed whether the basal PI3K activity in PC3 and LNCaP cells, which appears to be independent of p85 binding to RTKs or adaptor proteins, was mediated by a

particular p110 isoform. Significantly, siRNA mediated depletion of p110β, but not p110α or p110δ, decreased PI3K activity in serum starved PC3 cells (Fig. 9A). In contrast, PI3K pathway activation in PC3 cells in response to heregulin-β1 was suppressed by depletion of p110α, but not p110β or p110δ (Fig. 9B). In serum starved LNCaP cells, siRNA targeting both p110β and p110δ (which is expressed at higher levels in LNCaP versus PC3 cells) decreased PI3K activity, while p110α siRNA again had no effect (Fig. 9C). However, as in PC3 cells, only the p110α siRNA decreased PI3K pathway activation in response to heregulin-β1 (Fig. 9D). Finally, we addressed whether basal PI3K activity could be further suppressed by simultaneously silencing both p110β and δ. As shown in figure 9E and F, targeting both p110β and δ did not appear to be more effective. We presume this reflects an inability to completely silence both p110β and δ, but it remains possible that p110α can mediate some basal activity in the absence of other catalytic subunits. Taken together, these results indicate that basal PI3K activity in LNCaP and PC3 cells is mediated through p110β and p110δ (in LNCaP), and that this activity is independent of RTK mediated p85 recruitment.

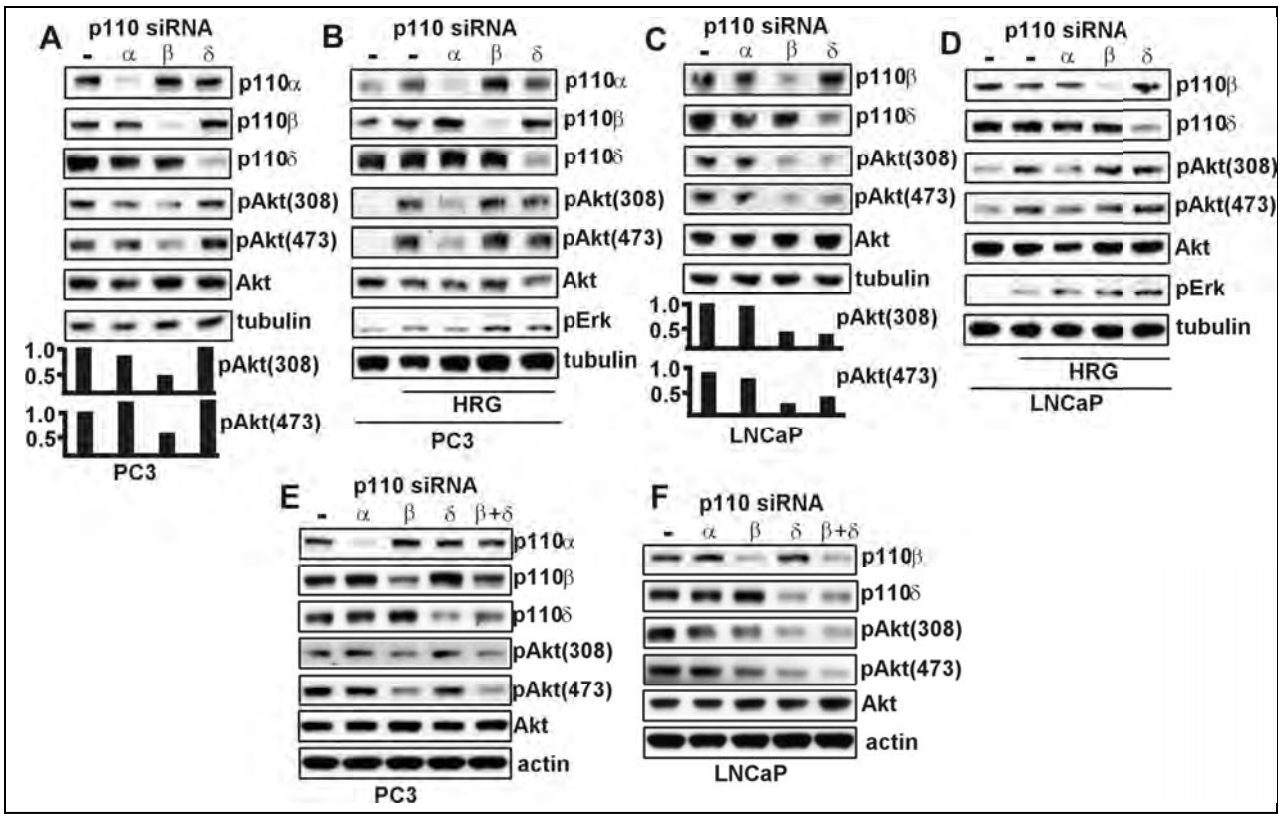

Figure 9. Distinct p110 isoforms mediate basal versus growth factor stimulated PI3K activity. PC3 (A) or LNCaP (C) cells in 24-well plates were transfected with siRNAs for each p110 isoform. After serum starvation for 1-2 days, cells were lysed and 10 μg of cell lysates were subjected to immunoblotting for each p110 isoform, pAkt, total Akt, or β-tubulin. Results are quantified in bar graphs, and are representative of 2-3 independent experiments for each cell type (in addition to results in 8E and 8F). PC3 (B) or LNCaP (D) transfected with siRNAs for each p110 isoform were serum starved for 1-2 days followed by HRG-β1 stimulation (100 ng/ml, 15 min). Cell lysates were then subjected to immunoblotting as indicated. (E) and (F),

PC3 or LNCaP cells respectively were transfected with siRNAs for each p110 isoform, or with both p110β and δ siRNA, and were then analyzed by immunoblotting after serum starvation for 2 days.

Aim 2. Test the hypothesis that receptor tyrosine kinase inhibitors can be used to block p85 membrane recruitment and suppress PI3 kinase activity *in vivo* in PCa xenografts.

Our data over the initial 2-2.5 years of the grant established that basal PI3 kinase activity in these PTEN deficient cells is not dependent on upstream receptor tyrosine kinase. However, PI3 kinase activity can still be increased by RTK signaling as shown above for heregulin-β1 stimulation in figure 9B and D. Therefore, we have most recently pursued an alternative approach which has been to identify the RTKs that are activated in PCa as it progresses. Using PCa xenograft models, we have generated matched castration sensitive and resistant tumors and derived cell lines based on the VCaP and LAPC4 models. Our preliminary studies indicate that RTKs including ErbB2, C-MET, and RET are activated in the castration resistant cells, and the effects of inhibitors on PI3 kinase activity and growth are currently being evaluated.

KEY RESEARCH ACCOMPLISHMENTS

- Established the central role of p110β in regulating basal PI3 kinase pathway activity in prostate cancer cells.

- Established the central role of p110α in regulating growth factor stimulated PI3 kinase pathway activity in prostate cancer cells.

REPORTABLE OUTCOMES

Cai,C., Portnoy,D.C., Wang,H., Jiang,X., Chen,S., and Balk,S.P. (2009). Androgen receptor expression in prostate cancer cells is suppressed by activation of epidermal growth factor receptor and ErbB2. Cancer Res. 69, 5202-5209

Jiang,X., Chen,S., Asara,J.M., and Balk,S.P. (2010). Phosphoinositide 3-kinase pathway activation in phosphate and tensin homolog (PTEN)-deficient prostate cancer cells is independent of receptor tyrosine kinases and mediated by the p110beta and p110delta catalytic subunits. J. Biol. Chem. 285, 14980-14989

CONCLUSION

Our findings in indicate that prostate epithelial cells that have sustained genetic or epigenetic loss of PTEN activity may be dependent initially on p110β (or possibly p110δ) for PI3K pathway activation and positive selection due to a relative lack of growth factors mediating activation of RTKs and p110α in the microenvironment of the fully developed adult human prostate. If this hypothesis is correct, then selective p110β inhibitors, or inhibitors of particular G protein coupled receptors or other upstream activators of p110β if present, may be most effective at early stages of PCa development. In contrast, as disease progression is likely associated with increased receptor tyrosine kinase stimulation and activation of p110α, the extent to which selective

inhibition of p110β will be effective in more advanced PCa is not clear and may be dependent on whether it still has a nonredundant downstream function.

APPENDICES

Two published manuscripts.

Androgen Receptor Expression in Prostate Cancer Cells Is Suppressed by Activation of Epidermal Growth Factor Receptor and ErbB2

Changmeng Cai, David C. Portnoy, Hongyun Wang, Xinnong Jiang, Shaoyong Chen, and Steven P. Balk

Cancer Biology Program/Hematology-Oncology Division, Department of Medicine, Beth Israel Deaconess Medical Center, Harvard Medical School, Boston, Massachusetts

Abstract

Prostate cancers (PCa) that relapse after androgen deprivation therapies [castration-resistant PCa (CRPC)] express high levels of androgen receptor (AR) and androgen-regulated genes, and evidence from several groups indicates that ErbB family receptor tyrosine kinases [epidermal growth factor (EGF) receptor (EGFR) and ErbB2] may contribute to enhancing this AR activity. We found that activation of these kinases with EGF and heregulin-β1 rapidly (within 8 hours) decreased expression of endogenous AR and androgen-regulated PSA in LNCaP PCa cells. AR expression was similarly decreased in LAPC4 and C4-2 cells, but not in the CWR22Rv1 PCa cell line. The rapid decrease in AR was not due to increased AR protein degradation and was not blocked by phosphatidylinositol 3-kinase (LY294002) or MEK (UO126) inhibitors. Significantly, AR mRNA levels in LNCaP cells were markedly decreased by EGF and heregulin-β1, and experiments with actinomycin D to block new mRNA synthesis showed that AR mRNA degradation was increased. AR mRNA levels were still markedly decreased by EGF and heregulin-β1 in LNCaP cells adapted to growth in androgen-depleted medium, although AR protein levels did not decline due to increased AR protein stability. These findings show that EGFR and ErbB2 can negatively regulate AR mRNA and may provide an approach to suppress AR expression in CRPC. [Cancer Res 2009;69(12):5202–9]

Introduction

Androgen receptor (AR) plays a central role in prostate cancer (PCa), with androgen deprivation therapies being the standard initial systemic treatment, but tumors eventually recur despite castrate androgen levels. These castration-resistant PCas (CRPC) express high levels of AR mRNA, AR protein, and androgen-regulated genes, indicating that AR transcriptional activity has been reactivated. One mechanism contributing to this reactivation is increased intratumoral androgen synthesis, but it seems clear that PCa adapts to androgen deprivation through multiple mechanisms that generate adequate AR activity despite castrate levels of circulating androgens (1–5). Evidence from several groups indicates that the ErbB family receptor tyrosine kinases ErbB1 [epidermal growth factor (EGF) receptor (EGFR)] and ErbB2 (HER2, Neu) contribute to enhancing AR activity in CRPC. Studies in PCa cell line and xenograft models have found increased EGFR or ErbB2 expression in tumors that relapse after castration, although this is not a consistent finding in patient samples and these receptors may also be enhanced by increased expression of ErbB ligands (6–14).

EGF can increase AR transactivation at low androgen levels, which may be mediated by increased expression or phosphorylation of the transcriptional coactivator protein TIF2/GRIP1 (15–18). The Ras-Raf-mitogen-activated protein kinase (MAPK) pathway and c-Src, which are activated downstream of EGFR, may also enhance AR responses to low levels of androgen (19–21). ErbB2 expression was increased in the LAPC4 xenograft model of CRPC, and a dual EGFR/ErbB2 inhibitor could reduce AR transcriptional activity and inhibit PCa xenograft growth after castration (6, 22). In CWR22 xenograft-derived CWR-R1 cells, heregulin stimulation of ErbB2 enhanced AR activity and cell growth (23). Other studies have shown that ErbB2 can enhance AR stability and that ErbB2 inhibition decreases AR DNA binding activity at low levels of androgen levels by a phosphatidylinositol 3-kinase (PI3K)–dependent, Akt-independent mechanism (6, 24, 25). In contrast, some studies indicate that ErbB2 enhances AR activity through the MAPK pathway or Akt (26, 27).

ErbB signaling also has been reported to negatively regulate AR expression and activity. In one study, EGF decreased AR mRNA and expression of androgen-regulated genes in LNCaP cells (28). In other studies, heparin binding EGF (HB-EGF) was found to decrease AR protein expression through activation of mTOR and decreased AR mRNA translation (29, 30). EGF also decreased PSA expression and secretion via the PI3K/Akt pathway in androgen-independent LNCaP-C81 cells (31). Finally, Akt in LNCaP cells may phosphorylate AR and enhance its ubiquitination by Mdm2 and degradation, but this seems to be dependent on cell passage number (32–36). Due to the significance of ErbB signaling in PCa, this study further examined how both EGF and heregulin-β1 regulate AR expression and activity in PCa cells.

Materials and Methods

Cell culture. LNCaP, LAPC4, C4-2, and CWR22-Rv1 cells were cultured in RPMI 1640/10% fetal bovine serum (FBS). HeLa and PC3-AR cells were cultured in DMEM/10% FBS. For DHT treatment, cells were grown to 50% to 60% confluence in medium with 5% charcoal/dextran-stripped serum (CSS; Hyclone) for 2 d before treatment.

Real-time reverse transcription–PCR. Primers and probes for quantitative real-time reverse transcription–PCR (RT-PCR) amplification were as follows: PSA forward, 5-GATGAAACAGGCTGTGCCG-3; PSA reverse, 5-CCTCACAGCTACCCACTGCA-3; PSA probe, 5-FAM-CAGGAACAAAAGCGTGATCTTGCTGGG-3; AR forward, 5′-GGAATTCCTGTGCATGAAA-3′; AR reverse, 5′-CGAAGTTCATCAAAGAATT-3′; AR probe, 5′-FAM-CTTCAGCATTATTCCAGTG-3′. Each reaction used 50 ng RNA and was normalized

Requests for reprints: Steven P. Balk, Beth Israel Deaconess Medical Center, Boston, MA 02215. Phone: 617-735-2065; Fax: 617-735-2050; E-mail: sbalk@bidmc.harvard.edu.

doi:10.1158/0008-5472.CAN-09-0026

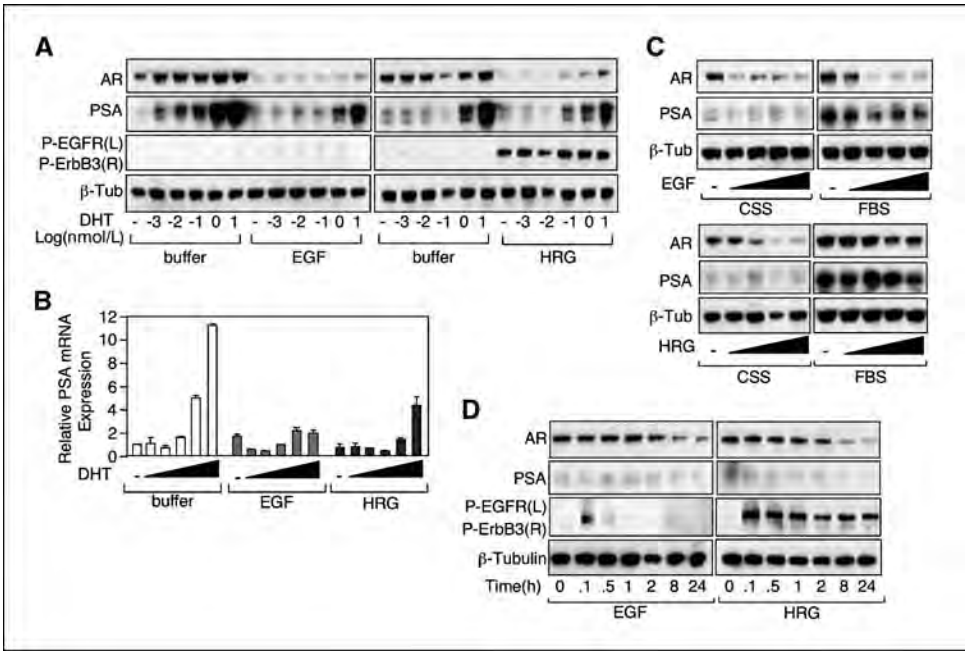

Figure 1. ErbB signaling decreases AR protein expression and transcriptional activity in LNCaP cells. LNCaP cells in 5% CSS medium were treated with 0, 10^{-3}, 10^{-2}, 10^{-1}, 1, or 10 nmol/L DHT in the absence or presence of 20 ng/mL EGF or 40 ng/mL heregulin-β1 for 24 h. *A,* equal amounts of total protein were immunoblotted for AR, PSA, phosphorylated EGFR (*P-EGFR*; Tyr^{845}) or phosphorylated ErbB3 (*P-ErbB3*; Tyr^{1289}). *B,* equal amounts of RNA were analyzed for PSA mRNA, with results normalized to an 18S RNA internal control. *C,* LNCaP cells, in either 5% CSS or 5% FBS medium, were treated with EGF or heregulin-β1 (0, 20, 40, 100, or 200 ng/mL) for 24 h and extracted proteins were then immunoblotted for AR or PSA expression. *D,* LNCaP cells in 5% CSS medium were treated with EGF or heregulin-β1 for 0, 0.1, 0.5, 2, 8, or 24 h and then immunoblotted for AR, PSA, phosphorylated EGFR (Tyr^{845}) or phosphorylated ErbB3 (Tyr^{1289}) expression. β-Tubulin was used as loading control.

by coamplification of 18S or glyceraldehyde-3-phosphate dehydrogenase (GAPDH) RNA.

Immunoblotting. Cell extracts were prepared by boiling for 15 min in 2% SDS buffer. Blots were probed with anti-PSA (1:3,000, polyclonal, BioDesign), anti-AR (1:2,000, polyclonal, Upstate), anti-FLAG (1:3,000, monoclonal, Sigma), anti-EGFR (1:1,000, polyclonal, Cell Signaling), anti–phosphorylated EGFR (Tyr^{845}; 1:1,000, polyclonal, Cell Signaling), anti–phosphorylated ErbB3 (Tyr^{1289}; 1:1,000, polyclonal, Cell Signaling), anti–phosphorylated AKT (Ser^{473}; 1:1,000, polyclonal, Cell Signaling), anti–phosphorylated ERK (Thr^{202}/Tyr^{204}; 1:1,000, polyclonal, Cell Signaling), anti–β-tubulin (1:2,000, monoclonal, Chemicon), or anti–β-actin (1:5,000, monoclonal, Abcom). Blots were developed with 1:5,000 antirabbit or antimouse secondary antibodies (Promega).

Results

ErbB signaling decreases endogenous AR protein expression and represses AR transcriptional activity in LNCaP cells. EGFR and ErbB2 signaling have been shown to increase AR activity, but most work has been done on transfected AR or using inhibitors, and it is unclear whether activation of ErbB receptors increases endogenous AR activity in PCa cells. As expected, AR protein and activity in LNCaP cells were significantly induced by DHT, based on increased expression of androgen-regulated PSA (Fig. 1*A*). In contrast, EGFR and ErbB2 activation with EGF and heregulin-β1, respectively, markedly suppressed PSA induction by DHT (Fig. 1*A, left* and *right*, respectively). Moreover, AR protein in the absence or presence of DHT was greatly reduced by EGF or heregulin-β1 (Fig. 1*A*). The activation of ErbB2 by heregulin-β1 was confirmed based on phosphorylation of ErbB3 (Fig. 1*A, right*). EGFR phosphorylation was not seen after 24 h of EGF treatment (Fig. 1*A, left*), consistent with its known rapid degradation after activation (see Fig. 1*D*). Confirming that EGF and heregulin-β1 were suppressing PSA transcription, androgen-induced PSA mRNA was markedly decreased by EGF and heregulin-β1 (Fig. 1*B*). These results indicated that activation of EGFR and ErbB2 were decreasing AR protein expression, leading to decreased AR activity (although both growth factors could stimulate proliferation in the absence or presence of androgen; data not shown).

To support this hypothesis, we next examined a range of EGF and heregulin-β1 concentrations. EGF at 20 ng/mL, which maximally stimulated EGFR activation (data not shown), markedly decreased AR protein at 24 hours in hormone-depleted medium (Fig. 1*C, left*) or in FBS medium (Fig. 1*C, right*), with a corresponding decrease in PSA protein. Heregulin-β1 similarly decreased AR expression, with the concentration required for maximal ErbB2 activation (40 ng/mL based on ErbB3 phosphorylation, data not shown) being consistent with the concentration that decreased AR and PSA protein (Fig. 1*C*). In time course experiments, EGFR activation (based on Tyr^{845} phosphorylation) could be detected after 0.1 hour but not at later times due to receptor down-regulation (Fig. 1*D, left*; data not shown). Robust ErbB3 phosphorylation was similarly detected at 0.1 hour but persisted for 24 hours (Fig. 1*D, right*). AR protein levels started to decline at ~2 hours, markedly decreased at 8 hours, and remained low after 24 hours.

ErbB signaling decreases AR in other PCa cell lines. To determine whether this repression of AR is LNCaP cell specific, we tested additional cells. LAPC4 cells have a wild-type AR and their growth is stimulated by androgen, but *in vitro* they express minimal PSA. Both EGF and heregulin-β1 in these cells slightly decreased the low levels of AR detected in the absence of DHT and greatly reduced AR in the presence of DHT (Fig. 2*A*). C4-2 cells were derived from a LNCaP xenograft that relapsed after castration, and the cultured cells have substantial AR activity (as assessed by PSA expression) in steroid hormone–depleted medium. EGF and heregulin-β1 both markedly decreased AR protein levels in these cells, and heregulin-β1 also suppressed PSA expression in response to DHT stimulation (Fig. 2*B*). Interestingly, PSA protein was decreased by EGF in the absence of exogenous DHT but was increased by EGF at 1 and 10 nmol/L DHT despite lower AR protein levels, possibly reflecting a marked increase in the activity of a coactivator in these cells (Fig. 2*B*). The AR in CWR22Rv1 cells has a point mutation and a duplicated exon 3, and these cells do not produce substantial PSA. AR protein in these cells could be increased by

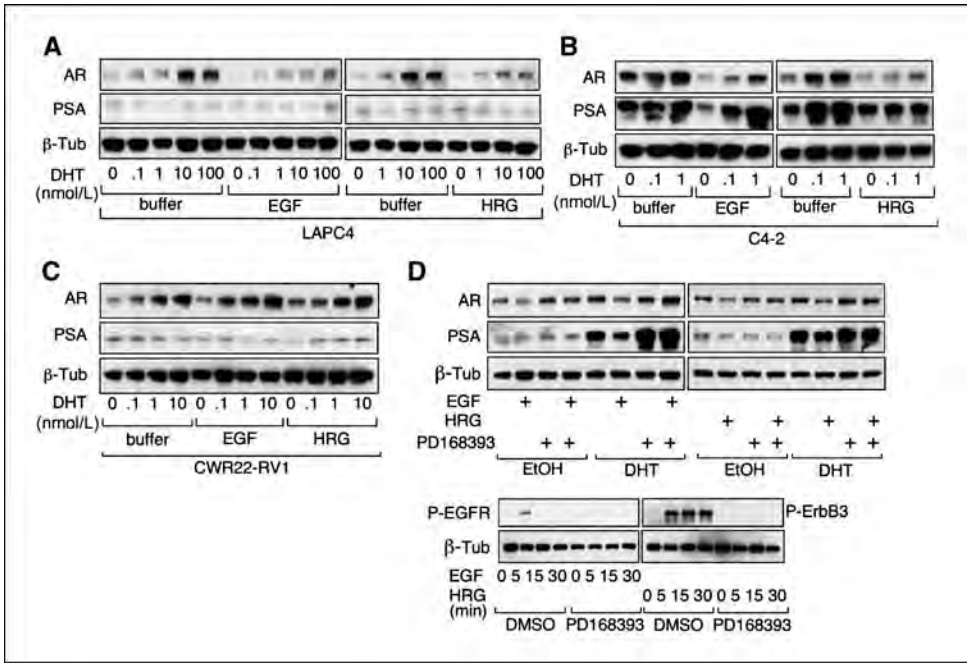

Figure 2. Effects of ErbB signaling on AR in other PCa cell lines. *A–C,* LAPC4, C4-2, or CWR22Rv1 cells in 5% CSS medium were treated with DHT (0–100 nmol/L) in the absence or presence of EGF or heregulin-β1 for 24 h, and equal amounts of protein were then immunoblotted for AR and PSA protein expression. *D, bottom,* LNCaP cells in 5% CSS medium were treated with EGF or heregulin-β1 in the absence or presence of PD168393 (10 μmol/L) for 0, 5, 15, or 30 min and then immunoblotted for phosphorylated EGFR (*P-EGFR*; Tyr^{845}) or phosphorylated ErbB3 (*P-ErbB3*; Tyr^{1289}) expression; *top,* LNCaP cells were treated with different combinations of PD168393, ethanol vehicle (0.1%), DHT (10 nmol/L), EGF (20 ng/mL), or heregulin-β1 (40 ng/mL) for 24 h and then immunoblotted for AR or PSA expression.

DHT, but EGF and heregulin-β1 had no clear effect on AR protein (Fig. 2*C*).

As expected, the irreversible EGFR/ErbB2 inhibitor PD168393 effectively blocked both EGFR ($pTyr^{845}$) and ErbB3 ($pTyr^{1289}$) activation in response to EGF and heregulin-β1, respectively (Fig. 2*D, bottom*). Moreover, EGF- and heregulin-β1–mediated repression of AR expression in LNCaP cells was abrogated by PD168393 (Fig. 2*D, top*). Interestingly, PD168393 increased androgen-induced PSA expression in the absence of growth factor stimulation, possibly due to the inhibition of basal EGFR or ErbB2 activity. Collectively, these data show that EGF, as well as heregulin-β1, markedly decrease both unliganded and liganded AR protein expression in several (but not all) AR- positive PCa cells.

ErbB signaling does not decrease expression of transfected AR. The results above are in contrast to some previous results with transfected AR (15, 18). Therefore, we used a triple-Flag tagged AR cDNA driven by a cytomegalovirus promoter to examine transfected AR in LNCaP and HeLa cells. In contrast to the above results with endogenous AR in LNCaP cells, EGF dramatically increased transiently transfected Flag-AR protein expression in the absence or presence of DHT (Fig. 3*A*). Heregulin-β1 also enhanced AR expression, but to a lesser extent than EGF. Similar results were obtained in HeLa cells (Fig. 3*B*). Because

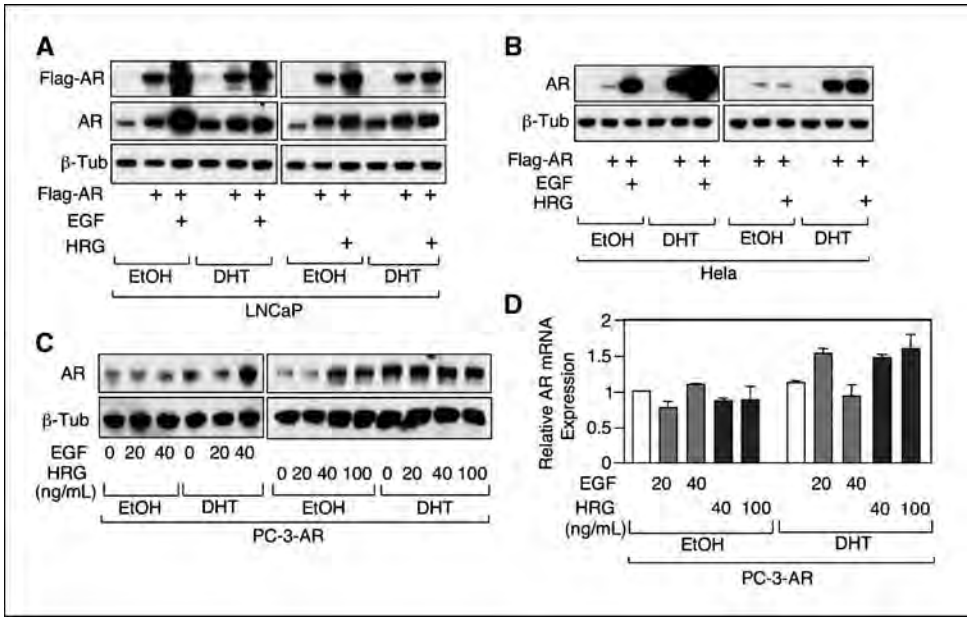

Figure 3. ErbB signaling does not decrease expression of transfected AR. *A,* LNCaP cells in 5% CSS medium were transfected with 0.25 μg Flag-AR for 24 h and then treated with EGF or heregulin-β1 in the absence or presence of DHT (10 nmol/L) for 24 h, and equal amounts of extracted proteins were immunoblotted for Flag (transfected AR) or total AR protein expression. *B,* HeLa cells in 5% CSS medium were transfected with 0.25 μg Flag-AR for 24 h, then treated with EGF or heregulin-β1 in the absence or presence of DHT (10 nmol/L) for 24 h, and immunoblotted for AR protein expression. *C,* PC-3 cells that stably express transfected AR (*PC-3-AR*) were grown in 5% CSS medium for 2 d, then treated with different concentration of EGF or heregulin-β1 in absence or presence of DHT (10 nmol/L) for 24 h, and immunoblotted for AR. β-Tubulin was used as loading control. *D,* AR mRNA expression in PC-3-AR cells treated as indicated for 24 h.

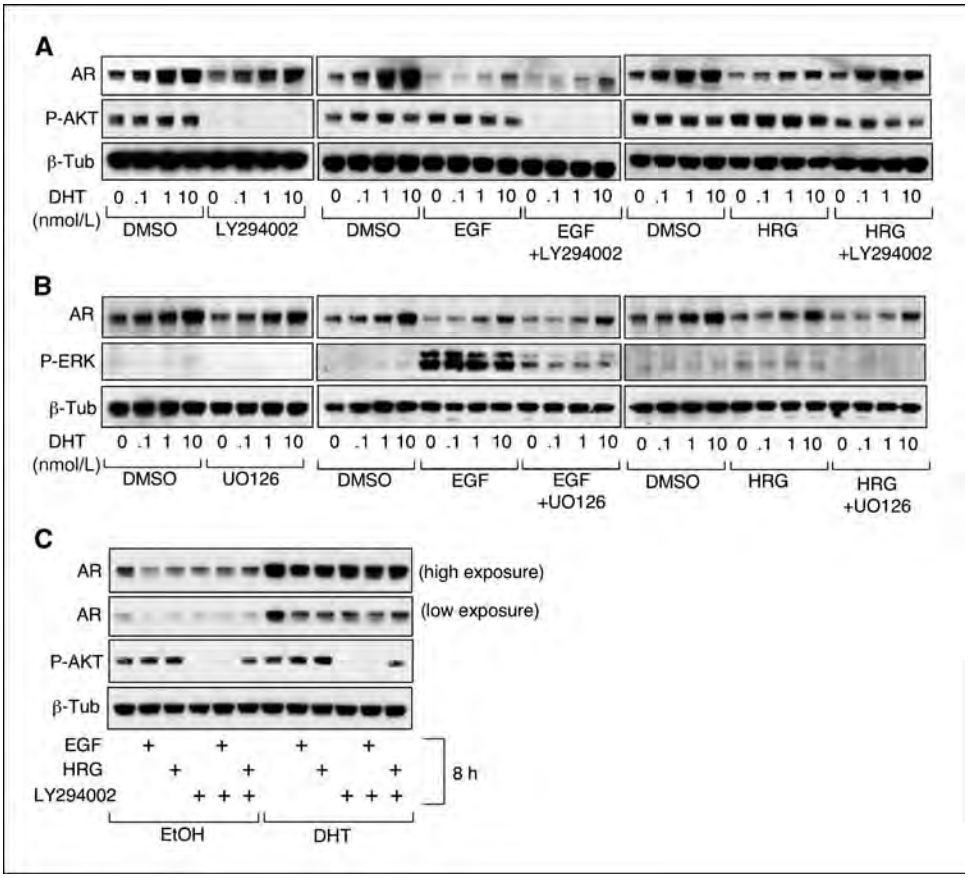

Figure 4. Contributions of PI3K and Erk to AR down-regulation by EGF and heregulin-β1. *A* and *B,* LNCaP cells in 5% CSS medium were treated with DHT (0-10 nmol/L), EGF (20 ng/mL), or heregulin-β1 (40 ng/mL), minus or plus LY294002 (40 μmol/L; *A*) or UO126 (10 μmol/L; *B*), as indicated for 24 h. Equal amounts of protein extracts were then immunoblotted for AR, phosphorylated AKT (*P-AKT*; Ser^{473}), or phosphorylated ERK (*P-ERK*; Thr^{202}/Tyr^{204}), with β-tubulin as a loading control. Cells receiving LY294002 or UO126 were pretreated with these inhibitors for 30 min before adding EGF or heregulin-β1. *C,* LNCaP cells were treated as above and analyzed by immunoblotting after 8 h.

transiently transfected cells express high levels of AR protein that may not be regulated by physiologic mechanisms, we also examined PC3 cells (an AR-negative PCa cell line) that were stably transfected with the AR expression vector. AR expression in these cells was modestly increased by EGF, and expression in the absence of DHT was markedly increased by heregulin-β1 (Fig. 3*C*). Significantly, AR mRNA levels in the PC3-AR cells were not markedly altered by these growth factors, indicating that AR protein translation or stability were being increased (Fig. 3*D*). In any case, as these data showed that endogenous versus transfected AR respond differently to ErbB pathway activation, we continued to focus on mechanisms regulating endogenous AR expression.

EGF decreases AR expression independently of PI3K and Erk activation, whereas PI3K contributes to AR down-regulation by heregulin-β1. We next examined whether the PI3K/Akt or Ras/Raf/Erk pathways, both of which can modulate AR function, were required for the EGF- or heregulin-β1–induced decrease in AR expression. LNCaP cells are PTEN deficient, so PI3K pathway activation is evidenced by high basal phosphorylated Akt, which was further enhanced by EGF (Fig. 4*A, left and middle*). Heregulin-β1 more strongly increased phosphorylated Akt levels, reflecting the robust recruitment and activation of PI3K by phosphorylated ErbB3 (Fig. 4*A, right*). The PI3K inhibitor LY294002 completely blocked the basal and EGF-stimulated Akt phosphorylation in LNCaP cells but did not prevent the marked decrease in AR protein in response to EGF (Fig. 4*A, left and middle*). In contrast, LY294002 substantially prevented the decrease in AR protein by heregulin-β1, despite only partially suppressing PI3K activation based on Akt phosphorylation (Fig. 4*A, right*).

Whereas EGF did not markedly enhanced PI3K activity in LNCaP cells, it very strongly activated the Ras/Raf/Erk pathway as evidenced by immunoblotting for phosphorylated Erk1/2 (Fig. 4*B, middle*). The MEK inhibitor UO126 blocked Erk activation in response to EGF but did not prevent the decrease in AR, indicating that EGF is not suppressing AR expression through Erk activation (Fig. 4*B, middle*). Heregulin-β1 only weakly stimulated Erk, and UO126 similarly did not block its ability to decrease AR expression (Fig. 4*B, right*).

As the above experiments examined AR after 24 hours, we next examined whether PI3K was contributing to the rapid decline in AR protein that can be clearly observed by 8 hours. Significantly, LY294002 did not prevent the marked decline in AR protein mediated by EGF or heregulin-β1 at 8 hours (Fig. 4*C*). We conclude that PI3K contributes to the decline in AR protein at 24 hours but that a distinct PI3K independent mechanism is mediating the rapid decline in AR protein between 2 and 8 hours in response to EGF and heregulin-β1.

AR protein degradation is not increased by EGF or heregulin-β1. To determine whether EGF or heregulin-β1 were increasing AR degradation, we used cycloheximide to inhibit new protein synthesis and assess AR protein stability. Cells in steroid-depleted medium (minus or plus DHT) were treated with cycloheximide alone or in conjunction with EGF or heregulin-β1, which were added 2 hours before the cycloheximide. This 2-hour pretreatment with growth factors was selected as AR protein expression is starting to decline at this time, and longer pretreatment results in much

lower baseline levels of AR that make half-life comparisons problematic. However, it should be noted that effects due to proteins that are induced by androgen after 2 hours may be missed. Cells were harvested at time 0 (immediately before cycloheximide addition) and at 4 to 24 hours. As seen in Fig. 5*A*, neither EGF nor heregulin-β1 substantially increased the rate of AR protein degradation at up to 8 hours, although degradation at 24 hours was increased. These results indicate that increased AR protein degradation does not account for the decline in AR protein levels that are observed within 8 hours of EGF or heregulin-β1 (see Fig. 1*D*) but may contribute to a further decline at later times.

EGF and heregulin-β1 increase degradation of AR mRNA. As AR protein degradation was not markedly increased by EGF or heregulin-β1 after up to 8 hours, we next assessed effects on AR mRNA. EGF markedly decreased endogenous AR mRNA by up to ~80% at 24 hours, whereas heregulin-β1 decreased AR mRNA by ~60% (Fig. 5*B, left*). These decreases occurred in the absence or presence of androgen. Moreover, they were observed within 4 hours, consistent with the rapid decline in AR protein (Fig. 5*B, right*). Significantly, AR mRNA levels were decreased by EGF and heregulin-β1 over a broad range of DHT concentrations, indicating that these growth factors are overriding mechanisms that enhance AR mRNA expression in response to androgen deprivation and low AR protein levels (37).

A regulatory element that represses AR gene transcription has been identified in the 5′ untranslated region (UTR), and it has been reported that a complex of Purα and hnRNPk binds this element and represses AR mRNA transcription (38–42). However, we did not detect increased expression of Purα or hnRNPk in response to EGF or heregulin-β1 (data not shown). Although this did not rule out posttranslational modifications in Purα or hnRNPk or decreased AR transcription by other mechanisms, we next examined AR mRNA stability. LNCaP cells (grown in medium minus or plus DHT) were pretreated with growth factors or vehicle for 8 hours, and actinomycin D was then added to block the new mRNA synthesis. In the absence of DHT or growth factors, AR mRNA had a half-life of ~8 hours, which was substantially decreased to ~4 hours in the presence of EGF or heregulin-β1 (Fig. 5*C, left*). EGF and heregulin-β1 similarly decreased AR mRNA half-life in the presence of DHT (Fig. 5*C, right*). It should be noted that the rate of AR mRNA degradation in the untreated cells increases abruptly after ~4 hours, which may

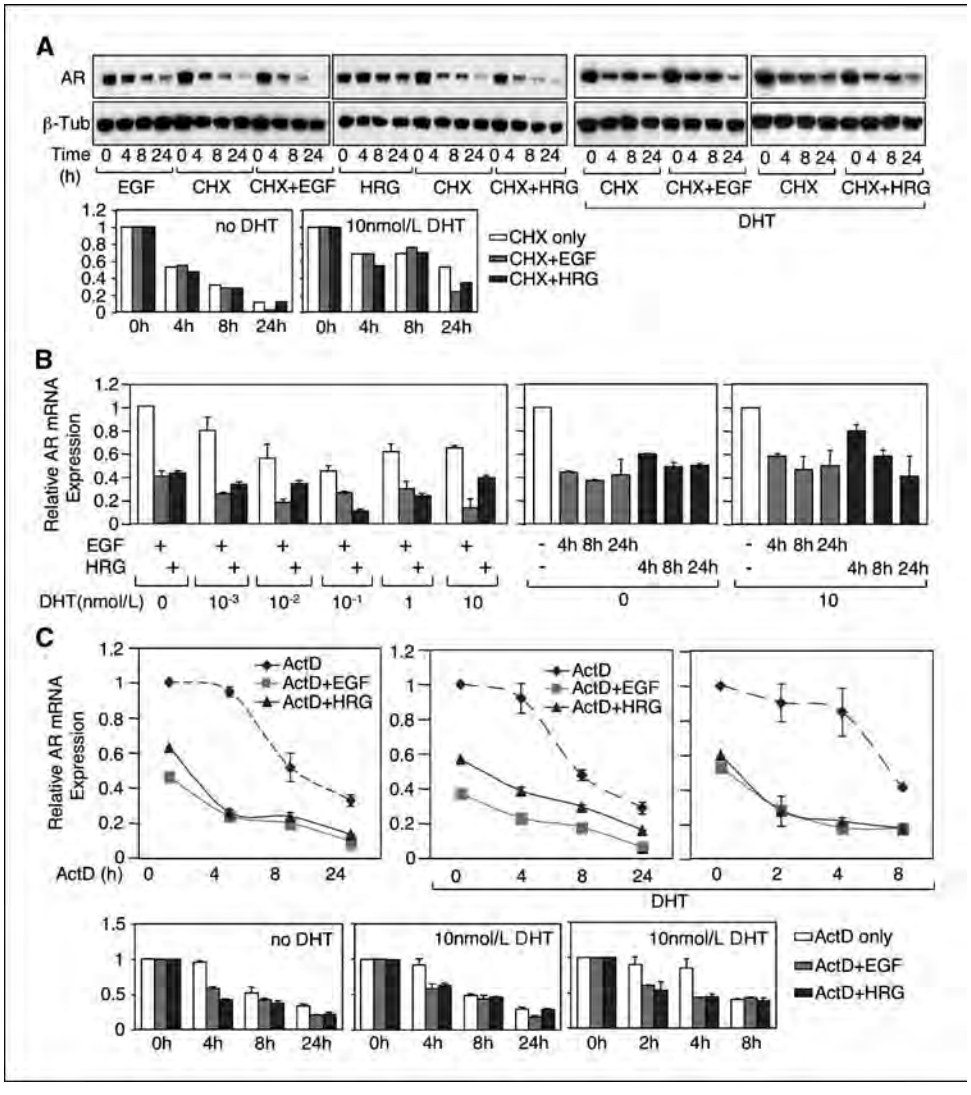

Figure 5. EGF and heregulin-β1 decrease AR mRNA levels and increase AR mRNA degradation. *A,* LNCaP cells in 5% CSS medium (*left*) or in 5% CSS medium with 10 nmol/L DHT (*right*) were treated with cycloheximide (10 ng/mL), EGF (20 ng/mL), and/or heregulin-β1 (40 ng/mL), as indicated, and then immunoblotted for AR. Cells were pretreated with EGF or heregulin-β1 at 2 h before cycloheximide treatment. *Bottom,* quantified results. *B,* LNCaP cells in 5% CSS were treated for 24 h (*left*) or over a 0- to 24-h time course (*right*) with 0 to 10 nmol/L DHT, minus or plus EGF (20 ng/mL) or heregulin-β1 (40 ng/mL). AR mRNA normalized to 18S RNA. *C,* LNCaP cells in 5% CSS medium (*left*) or in 5% CSS medium with 10 nmol/L DHT (*right*) were treated with actinomycin D (10 μmol/L), minus or plus EGF (20 ng/mL) or heregulin-β1 (40 ng/mL) for 0, 2, 4, 8, or 24 (8 h pretreatment with growth factors, the 0–24 h and 0–8 h time courses with DHT are from separate experiments). Equal amounts of RNA were then analyzed for AR mRNA expression (normalized to GAPDH mRNA) by real-time RT-PCR. *Bottom,* quantified results, with all values at time 0 being normalized to 1.

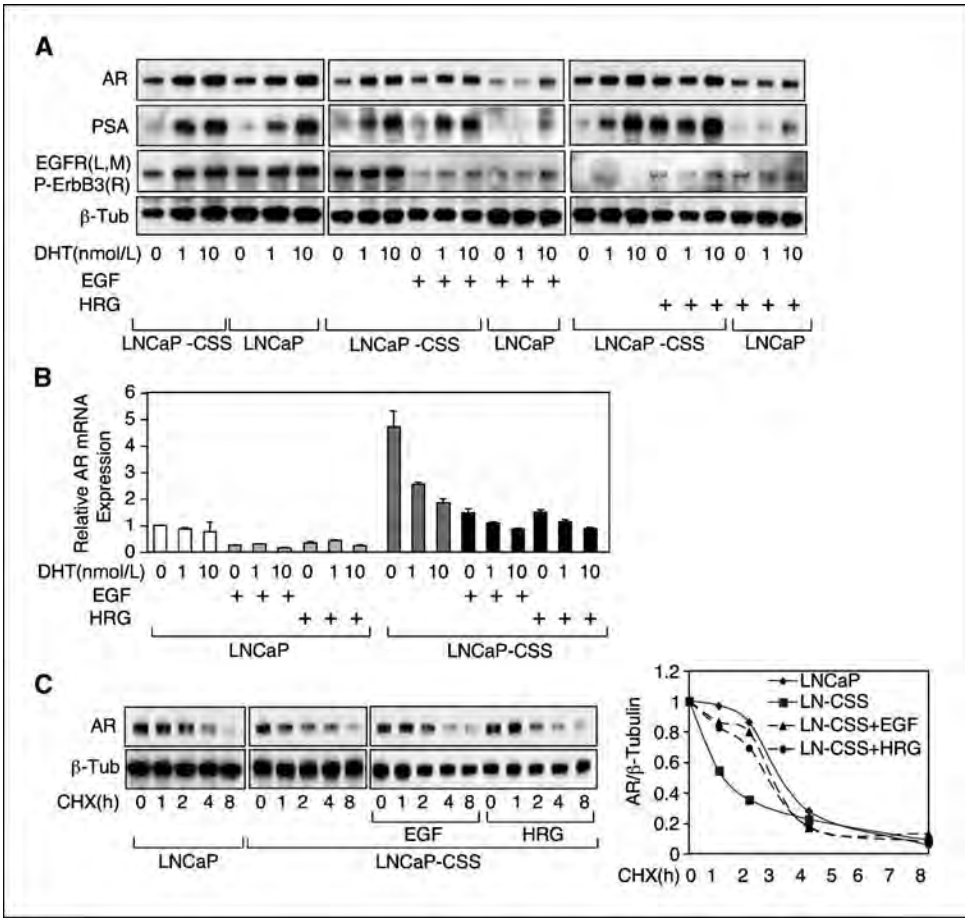

Figure 6. EGF and heregulin-β1 increase AR protein stability in LNCaP cells adapted to growth in androgen-depleted medium. *A* and *B,* LNCaP cells were cultured in either 10% CSS medium (*LNCaP-CSS*) or 10% FBS medium for ~4 to wk. The LNCaP-CSS and control LNCaP cells were then grown in 5% CSS medium for 2 d and then treated for 24 h with 0, 1, or 10 nmol/L DHT in the absence or presence of EGF (20 ng/mL) or heregulin-β1 (40 ng/mL). *A,* equal amounts of protein were immunoblotted for AR, PSA, EGFR (*left*), or phosphorylated ErbB3 (*P-ErbB3*; Tyr^{1289}; *right*) expression. *B,* equal amounts of RNA were analyzed for AR mRNA by real-time RT-PCR (normalized using internal GAPDH control). *C,* control LNCaP and LNCaP-CSS cells in 5% CSS medium were treated with cycloheximide (10 ng/mL), minus or plus EGF or heregulin-β1, for 0, 1, 2, 4, or 8 h, and equal amounts of protein were then immunoblotted for AR. *Right,* quantification of AR normalized to β-tubulin.

reflect an actinomycin D–induced degradative pathway and result in an underestimation of AR mRNA stability in the untreated cells. In any case, the data indicate that increased mRNA degradation contributes to the decline in AR mRNA in response to EGF and heregulin-β1.

EGF and heregulin-β1 increase AR protein stability in LNCaP cells adapted to growth in androgen-depleted medium. Studies using patient samples and xenograft models have shown that AR mRNA levels are high in CRPC and are increased relative to primary untreated PCa (4, 43–45). Therefore, as EGFR and ErbB2 activities may be increased in CRPC, we considered whether EGF and heregulin-β1 would still suppress AR mRNA levels in PCa cells adapted to grow under androgen-deprived conditions. To test this hypothesis, we changed the growing condition of LNCaP cells from medium with normal FBS to medium with steroid-depleted CSS.

Short-term culturing (1 week) in CSS medium did not significantly affect the suppression of AR protein by EGF or heregulin-β1 (data not shown), but a longer-term culture (~4–6 weeks) in CSS medium did alter this response. As shown in Fig. 6*A*, AR protein levels in the LNCaP-CSS cells (cells grown in CSS medium for ~4–6 weeks), in the absence or presence of DHT, were not decreased by EGF or heregulin-β1 (Fig. 6*A*). Immunoblotting for EGFR (which is rapidly down-regulated in response to activation) and pErbB3 confirmed that both the LNCaP and LNCaP-CSS cells were stimulated by EGF and heregulin-β1. Interestingly, in the LNCaP-CSS cells, heregulin-β1 stimulated the expression of PSA in the absence of added DHT (Fig. 6*A, right*), consistent with the conclusion that ErbB2 stimulation can, under some conditions, enhance AR transcriptional activity in the absence of androgens or at low androgen levels (6, 23–25).

Significantly, AR mRNA levels were markedly increased in the LNCaP-CSS versus the parental LNCaP cells and rapidly declined in response to DHT (Fig. 6*B*). However, although EGF and heregulin-β1 did not decrease AR protein levels in the LNCaP-CSS cells, they both still markedly decreased AR mRNA levels in the absence and presence of DHT (Fig. 6*B*). Therefore, as these growth factors were still decreasing AR mRNA but not AR protein, we examined AR protein stability in the LNCaP versus LNCaP-CSS cells (pretreated for 2 hours with EGF or heregulin-β1 before addition of cycloheximide at time 0). AR protein was less stable (half-life ~1 hour) in the LNCaP-CSS cells grown in CSS medium than in the parental LNCaP cells in the same medium (half-life ~2.0 hours; Fig. 6*C*), indicating that the LNCaP-CSS cells adapted to androgen deprivation primarily by increasing AR mRNA levels. However, in contrast to the parental LNCaP cells (see above), both EGF and heregulin-β1 increased AR protein half-life in LNCaP-CSS cells from ~1 to ~3 hours (Fig. 6*C*, quantified in the *right*). This result indicates that increasing AR protein stability through activation of EGFR or ErbB2 is a mechanism that may contribute to maintaining AR protein expression in CRPC, particularly if it can become uncoupled from the down-regulation of AR mRNA.

Discussion

Previous studies indicate that stimulation of EGFR and ErbB2 can enhance AR stability and transcriptional function and may contribute to AR activity in CRPC (6, 15, 18, 22–25, 27). We initially examined LNCaP PCa cells to further define the molecular basis for these effects on AR and found that stimulation with both EGF and heregulin-β1 rapidly decreased expression of AR protein and the androgen-regulated *PSA* gene over a broad range of DHT concentrations. This decrease in AR protein was also observed in LAPC4 and C4-2 cells but not in CWR22Rv1 cells. Consistent with the latter result, AR protein in another CWR22-derived cell line (CWR-R1) was not changed in response to EGF or heregulin (18, 23). The rapid AR down-regulation in response to EGF and heregulin-β1 was not prevented by UO126 or LY294002, indicating that it was not mediated through the Erk or PI3K pathways. Moreover, AR protein degradation was not rapidly enhanced by EGF or heregulin-β1. In contrast, AR mRNA levels were rapidly decreased by both EGF and heregulin-β1 over a broad range of DHT concentrations. Decreased AR transcription likely contributes to this decrease, but AR mRNA degradation was also increased in response to EGF and heregulin-β1. Taken together these findings show that EGFR and ErbB2 activation, while having multiple effects on AR activity through diverse mechanisms, markedly decrease AR mRNA expression and increase AR mRNA degradation.

The AR has a long 3′ UTR, which contains a highly conserved UC-rich region implicated in the regulation of mRNA stability (46). Therefore, EGFR or ErbB2 may regulate expression of RNA binding proteins that interact with this UC-rich region (47). Decreased AR mRNA transcription also likely contributes to the marked decrease in AR mRNA levels in response to EGF and heregulin-β1. AR transcription may be regulated by multiple factors, including a suppressor element in the AR 5′ UTR (40, 48–52). Further studies are clearly needed to define the precise mechanisms by which EGF and heregulin-β1 are enhancing AR mRNA degradation and to assess their effects on AR mRNA transcription.

Previous studies indicated that EGF could enhance AR activity and that ErbB2 could enhance AR stability and responses to low levels of androgen (6, 15–18, 23–27). However, other studies in LNCaP cells found that EGF or HB-EGF decrease AR expression, consistent with the findings in the current study (28–31). One factor that may contribute to differences between studies is that results in some cases are based on transfected AR (15, 18). Another factor is the use of EGFR/ErbB2 inhibitors in some studies to examine the effects of basal growth factor receptor activity on the endogenous AR versus the use of EGF and heregulin-β1 to examine the response to EGFR/ErbB2 activation in the current study (22, 24, 25). Whereas one might conclude that decreased AR activity in response to EGFR/ErbB2 inhibitors would predict increased AR activity in response to EGF and heregulin-β1, this may not be the case as the rapid high-level stimulation with EGF/heregulin-β1 may be eliciting distinct responses. Therefore, whereas the results in this study identify a novel mechanism by which EGFR and ErbB2 can suppress AR expression, the overall response to activation or inhibition of these receptors *in vivo* may be variable and not readily predictable due to interactions between multiple downstream pathways.

As noted above, EGFR and ErbB2 activate multiple downstream pathways that may directly or indirectly modulate AR expression and function. One example in this study was that EGF treatment caused a strong increase in DHT-stimulated PSA expression in C4-2 cells despite a decrease in AR protein. This is consistent with a previous study showing that EGF can increase phosphorylation and activity of the p160 transcriptional coactivator SRC-2/TIF2/GRIP1 (18). A second example was the ability of the PI3K inhibitor LY294002 to partially block the heregulin-β1–stimulated decline in AR protein at 24 hours (but not 8 hours), which is consistent with a previous study showing that mTOR activation in response to HB-EGF caused a decrease in AR translation (30). A third example is that heregulin-β1 increased AR protein stability and stimulated PSA expression in the LNCaP-CSS cells in the absence of added DHT. These effects are similar to those observed in LAPC4 cells adapted to grow under castrate conditions, although their molecular basis remains to be defined (24). Importantly, the LNCaP-CSS cells also adapted to androgen deprivation by increasing their AR mRNA to maintain AR protein levels. However, heregulin-β1 still markedly decreased AR mRNA levels in these cells so that heregulin-β1 did not increase AR protein levels. It will be important to determine in CRPC patients whether the mechanisms that decrease AR mRNA in response to EGF/heregulin-β1 are uncoupled from mechanisms that enhance AR transcriptional activity and to determine whether these former mechanisms can be targeted by drugs to prevent the increase in AR mRNA levels that occurs in CRPC.

Disclosure of Potential Conflicts of Interest

No potential conflicts of interest were disclosed.

Acknowledgments

Received 1/5/09; revised 3/31/09; accepted 4/10/09; published OnlineFirst 6/2/09.

Grant support: NIH, Department of Defense, Dana-Farber/Harvard Cancer Center Prostate Cancer Specialized Programs of Research Excellence, and Prostate Cancer Foundation (S.P. Balk); postdoctoral fellowships from Department of Defense (C. Cai, H. Wang, and X. Jiang); and NIH K99/R00 award (S. Chen).

The costs of publication of this article were defrayed in part by the payment of page charges. This article must therefore be hereby marked *advertisement* in accordance with 18 U.S.C. Section 1734 solely to indicate this fact.

References

1. Mohler JL, Gregory CW, Ford OH, et al. The androgen axis in recurrent prostate cancer. Clin Cancer Res 2004; 10:440–8.
2. Titus MA, Schell MJ, Lih FB, Tomer KB, Mohler JL. Testosterone and dihydrotestosterone tissue levels in recurrent prostate cancer. Clin Cancer Res 2005;11: 4653–7.
3. Montgomery RB, Mostaghel EA, Vessella R, et al. Maintenance of intratumoral androgens in metastatic prostate cancer: a mechanism for castration-resistant tumor growth. Cancer Res 2008;68:4447–54.
4. Stanbrough M, Bubley GJ, Ross K, et al. Increased expression of genes converting adrenal androgens to testosterone in androgen-independent prostate cancer. Cancer Res 2006;66:2815–25.
5. Attard G, Reid AH, Yap TA, et al. Phase I clinical trial of a selective inhibitor of CYP17, abiraterone acetate, confirms that castration-resistant prostate cancer commonly remains hormone driven. J Clin Oncol 2008;26: 4563–71.
6. Craft N, Shostak Y, Carey M, Sawyers CL. A mechanism for hormone-independent prostate cancer through modulation of androgen receptor signaling by the HER-2/neu tyrosine kinase [see comments]. Nat Med 1999;5:280–5.
7. Berger R, Lin DI, Nieto M, et al. Androgen-dependent regulation of Her-2/neu in prostate cancer cells. Cancer Res 2006;66:5723–8.
8. Signoretti S, Montironi R, Manola J, et al. Her-2-neu expression and progression toward androgen independence in human prostate cancer. J Natl Cancer Inst 2000;92:1918–25.
9. Shi Y, Brands FH, Chatterjee S, et al. Her-2/neu expression in prostate cancer: high level of expression associated with exposure to hormone therapy and androgen independent disease. J Urol 2001;166:1514–9.
10. Reese DM, Small EJ, Magrane G, Waldman FM, Chew K, Sudilovsky D. HER2 protein expression and gene amplification in androgen-independent prostate cancer. Am J Clin Pathol 2001;116:234–9.
11. Calvo BF, Levine AM, Marcos M, et al. Human epidermal receptor-2 expression in prostate cancer. Clin Cancer Res 2003;9:1087–97.

12. Savinainen KJ, Saramaki OR, Linja MJ, et al. Expression and gene copy number analysis of ERBB2 oncogene in prostate cancer. Am J Pathol 2002;160:339–45.

13. Osman I, Scher HI, Drobnjak M, et al. HER-2/neu (p185neu) protein expression in the natural or treated history of prostate cancer. Clin Cancer Res 2001;7: 2643–7.

14. Leung HY, Weston J, Gullick WJ, Williams G. A potential autocrine loop between heregulin-α and erbB-3 receptor in human prostatic adenocarcinoma. Br J Urol 1997;79:212–6.

15. Culig Z, Hobisch A, Cronauer MV, et al. Androgen receptor activation in prostatic tumor cell lines by insulin-like growth factor-I, keratinocyte growth factor, and epidermal growth factor. Cancer Res 1994;54:5474–8.

16. Reinikainen P, Palvimo JJ, Janne OA. Effects of mitogens on androgen receptor-mediated transactivation. Endocrinology 1996;137:4351–7.

17. Orio F, Jr., Terouanne B, Georget V, et al. Potential action of IGF-1 and EGF on androgen receptor nuclear transfer and transactivation in normal and cancer human prostate cell lines. Mol Cell Endocrinol 2002;198: 105–14.

18. Gregory CW, Fei X, Ponguta LA, et al. Epidermal growth factor increases coactivation of the androgen receptor in recurrent prostate cancer. J Biol Chem 2004; 279:7119–30.

19. Weber MJ, Gioeli D. Ras signaling in prostate cancer progression. J Cell Biochem 2004;91:13–25.

20. Kraus S, Gioeli D, Vomastek T, Gordon V, Weber MJ. Receptor for activated C kinase 1 (RACK1) and Src regulate the tyrosine phosphorylation and function of the androgen receptor. Cancer Res 2006;66:11047–54.

21. Guo Z, Dai B, Jiang T, et al. Regulation of androgen receptor activity by tyrosine phosphorylation. Cancer Cell 2006;10:309–19.

22. Mellinghoff IK, Tran C, Sawyers CL. Growth inhibitory effects of the dual ErbB1/ErbB2 tyrosine kinase inhibitor PKI-166 on human prostate cancer xenografts. Cancer Res 2002;62:5254–9.

23. Gregory CW, Whang YE, McCall W, et al. Heregulin-induced activation of HER2 and HER3 increases androgen receptor transactivation and CWR-R1 human recurrent prostate cancer cell growth. Clin Cancer Res 2005;11:1704–12.

24. Mellinghoff IK, Vivanco I, Kwon A, Tran C, Wongvipat J, Sawyers CL. HER2/neu kinase-dependent modulation of androgen receptor function through effects on DNA binding and stability. Cancer Cell 2004;6:517–27.

25. Liu Y, Majumder S, McCall W, et al. Inhibition of HER-2/neu kinase impairs androgen receptor recruitment to the androgen responsive enhancer. Cancer Res 2005;65:3404–9.

26. Yeh S, Lin HK, Kang HY, Thin TH, Lin MF, Chang C. From HER2/Neu signal cascade to androgen receptor and its coactivators: a novel pathway by induction of androgen target genes through MAP kinase in prostate cancer cells. Proc Natl Acad Sci U S A 1999;96:5458–63.

27. Wen Y, Hu MC, Makino K, et al. HER-2/neu promotes androgen-independent survival and growth of prostate cancer cells through the Akt pathway. Cancer Res 2000; 60:6841–5.

28. Henttu P, Vihko P. Growth factor regulation of gene expression in the human prostatic carcinoma cell line LNCaP. Cancer Res 1993;53:1051–8.

29. Adam RM, Kim J, Lin J, et al. Heparin-binding epidermal growth factor-like growth factor stimulates androgen-independent prostate tumor growth and antagonizes androgen receptor function. Endocrinology 2002;143:4599–608.

30. Cinar B, De Benedetti A, Freeman MR. Post-transcriptional regulation of the androgen receptor by Mammalian target of rapamycin. Cancer Res 2005;65: 2547–53.

31. Hakariya T, Shida Y, Sakai H, Kanetake H, Igawa T. EGFR signaling pathway negatively regulates PSA expression and secretion via the PI3K-Akt pathway in LNCaP prostate cancer cells. Biochem Biophys Res Commun 2006;342:92–100.

32. Lin HK, Yeh S, Kang HY, Chang C. Akt suppresses androgen-induced apoptosis by phosphorylating and inhibiting androgen receptor. Proc Natl Acad Sci U S A 2001;98:7200–5.

33. Lin HK, Wang L, Hu YC, Altuwaijri S, Chang C. Phosphorylation-dependent ubiquitylation and degradation of androgen receptor by Akt require Mdm2 E3 ligase. EMBO J 2002;21:4037–48.

34. Lin HK, Hu YC, Yang L, et al. Suppression versus induction of androgen receptor functions by the phosphatidylinositol 3-kinase/Akt pathway in prostate cancer LNCaP cells with different passage numbers. J Biol Chem 2003;278:50902–7.

35. Gaughan L, Logan IR, Neal DE, Robson CN. Regulation of androgen receptor and histone deacetylase 1 by Mdm2-mediated ubiquitylation. Nucleic Acids Res 2005; 33:13–26.

36. Taneja SS, Ha S, Swenson NK, et al. Cell-specific regulation of androgen receptor phosphorylation *in vivo*. J Biol Chem 2005;280:40916–24.

37. Krongrad A, Wilson CM, Wilson JD, Allman DR, McPhaul MJ. Androgen increases androgen receptor protein while decreasing receptor mRNA in LNCaP cells. Mol Cell Endocrinol 1991;76:79–88.

38. Kumar MV, Jones EA, Grossmann ME, Blexrud MD, Tindall DJ. Identification and characterization of a suppressor element in the 5′-flanking region of the mouse androgen receptor gene. Nucleic Acids Res 1994;22: 3693–98.

39. Grossmann ME, Lindzey J, Kumar MV, Tindall DJ. The mouse androgen receptor is suppressed by the 5′-untranslated region of the gene. Mol Endocrinol 1994;8: 448–55.

40. Wang LG, Johnson EM, Kinoshita Y, et al. Androgen receptor overexpression in prostate cancer linked to Purα loss from a novel repressor complex. Cancer Res 2008;68:2678–88.

41. Inoue T, Leman ES, Yeater DB, Getzenberg RH. The potential role of purine-rich element binding protein (PUR) α as a novel treatment target for hormone-refractory prostate cancer. Prostate 2008;68:1048–56.

42. Wang LG, Ossowski L, Ferrari AC. Androgen receptor level controlled by a suppressor complex lost in an androgen-independent prostate cancer cell line. Oncogene 2004;23:5175–84.

43. Taplin ME, Bubley GJ, Shuster TD, et al. Mutation of the androgen-receptor gene in metastatic androgen-independent prostate cancer. N Engl J Med 1995;332: 1393–8.

44. Holzbeierlein J, Lal P, LaTulippe E, et al. Gene expression analysis of human prostate carcinoma during hormonal therapy identifies androgen-responsive genes and mechanisms of therapy resistance. Am J Pathol 2004;164:217–27.

45. Chen CD, Welsbie DS, Tran C, et al. Molecular determinants of resistance to antiandrogen therapy. Nat Med 2004;10:33–9.

46. Yeap BB, Wilce JA, Leedman PJ. The androgen receptor mRNA. BioEssays 2004;26:672–82.

47. Yeap BB, Voon DC, Vivian JP, et al. Novel binding of HuR and poly(C)-binding protein to a conserved UC-rich motif within the 3′-untranslated region of the androgen receptor messenger RNA. J Biol Chem 2002;277: 27183–92.

48. Kumar MV, Jones EA, Felts SJ, et al. Characterization of a TPA-response element in the 5′-flanking region of the androgen receptor gene. J Androl 1998;19: 595–602.

49. Yang L, Xie S, Jamaluddin MS, et al. Induction of androgen receptor expression by phosphatidylinositol 3-kinase/Akt downstream substrate, FOXO3a, and their roles in apoptosis of LNCaP prostate cancer cells. J Biol Chem 2005;280:33558–65.

50. Lindzey J, Grossmann M, Kumar MV, Tindall DJ. Regulation of the 5′-flanking region of the mouse androgen receptor gene by cAMP and androgen. Mol Endocrinol 1993;7:1530–40.

51. Mizokami A, Yeh SY, Chang C. Identification of 3′,5′-cyclic adenosine monophosphate response element and other *cis*-acting elements in the human androgen receptor gene promoter. Mol Endocrinol 1994;8:77–88.

52. Grad JM, Dai JL, Wu S, Burnstein KL. Multiple androgen response elements and a Myc consensus site in the androgen receptor (AR) coding region are involved in androgen-mediated up-regulation of AR messenger RNA. Mol Endocrinol 1999;13:1896–911.

THE JOURNAL OF BIOLOGICAL CHEMISTRY VOL. 285, NO. 20, pp. 14980–14989, May 14, 2010

Phosphoinositide 3-Kinase Pathway Activation in Phosphate and Tensin Homolog (PTEN)-deficient Prostate Cancer Cells Is Independent of Receptor Tyrosine Kinases and Mediated by the p110β and p110δ Catalytic Subunits*[S]

Received for publication, November 16, 2009, and in revised form, March 9, 2010 Published, JBC Papers in Press, March 15, 2010, DOI 10.1074/jbc.M109.085696

Xinnong Jiang[‡1], **Sen Chen**[‡], **John M. Asara**[§2], **and Steven P. Balk**[‡3]

From the [‡]*Hematology-Oncology and* [§]*Signal Transduction Divisions, Department of Medicine, Beth Israel Deaconess Medical Center, Harvard Medical School, Boston, Massachusetts 02215*

Class IA phosphoinositide 3-kinase (PI3K) p110 catalytic subunits are activated upon Src homology 2 domain-mediated binding of their p85 regulatory subunits to tyrosine-phosphorylated pY*XX*M motifs in receptor tyrosine kinases (RTKs) or adaptor proteins. The PI3K pathway is activated by phosphate and tensin homolog (PTEN) loss in most prostate cancers (PCa), but the contribution of upstream RTKs that may be targeted therapeutically has not been assessed. Immunoblotting of p85-associated proteins in serum-starved PTEN-deficient LNCaP and C4-2 PCa cells showed a small set of discrete tyrosine-phosphorylated proteins, but these proteins were not recognized by an anti-pY*XX*M motif antibody and were not found in PTEN-deficient PC3 PCa cells. LC/MS/MS using label-free proteomics and immunoblotting showed that p85 was associated primarily with p110β and p110δ. An interaction with ErbB3 was also detected but was independent of ErbB3 tyrosine phosphorylation and was not required for basal PI3K activity. Basal tyrosine phosphorylation of p110β and p110δ could be blocked by c-Src inhibitors, but this did not suppress PI3K activity, which was similarly independent of Ras. Basal PI3K activity was mediated by p110β in PC3 cells and by both p110β and p110δ in LNCaP cells, whereas p110α was required for PI3K activation in response to RTK stimulation by heregulin-β1. These findings show that basal PI3K activity in PTEN-deficient PCa cells is RTK-independent and can be mediated by p110β and p110δ. Increased p110β expression in PCa may be required for RTK-independent PI3K pathway activation in adult prostate epithelium with genetic or epigenetic PTEN down-regulation.

The class I phosphoinositide 3-kinases (PI3Ks)[4] produce phosphatidylinositol 3,4,5-trisphosphate, which recruits proteins containing phosphatidylinositol 3,4,5-trisphosphate-binding pleckstrin homology domains to the plasma membrane (1). This class can be further divided into class IA PI3Ks, which consist of a p85 regulatory subunit (p85α, p85β, or p55γ) and a p110 catalytic subunit (p110α, p110β, or p110δ) and class IB PI3Ks that have a p101 regulatory subunit and a p110γ catalytic subunit. The class IA PI3Ks are generally activated by a subset of receptor tyrosine kinases (RTKs), which undergo tyrosine phosphorylation in response to ligand binding. The class IA PI3Ks are then recruited to the membrane by their p85 regulatory subunits, which contain SH2 domains that bind to pY*XX*M motifs in tyrosine-phosphorylated RTKs or adaptor proteins that are tyrosine-phosphorylated by RTKs (2). In addition to mediating membrane recruitment, p85 inhibits the catalytic activity of the p110 subunit, and inhibition is relieved upon binding to RTKs or adaptor proteins (3). This PI3K pathway is negatively regulated by phosphate and tensin homolog (PTEN), which functions as a phosphatidylinositol 3,4,5-trisphosphate phosphatase whose loss and subsequent activation of PI3K signaling makes a major contribution to many cancers (4–7). Studies of PTEN gene deletion, mutations, and protein expression have shown that PTEN is lost in a large fraction of metastatic prostate cancers (PCa) and in many aggressive primary PCa and that partial loss of PTEN by genetic or epigenetic mechanisms probably contributes to PCa development (8–12). Studies in mice have confirmed that PTEN loss promotes the development of PCa and that PTEN is haploinsufficient because loss of one allele can drive PCa when combined with other genetic lesions (13–15).

Although PTEN loss appears to be the most common overall genetic mechanism for activation of PI3K in tumors, large scale sequencing efforts have identified activating mutations or amplification of p110α as another common mechanism for PI3K pathway activation (16). Significantly, although activating

* This work was supported, in whole or in part, by National Institutes of Health Grants Prostate SPORE P50 CA90381 and P01CA89021 (to S. P. B.). This work was also supported by United States Department of Defense Grant PC073779 (to S. P. B.).

[S] The on-line version of this article (available at http://www.jbc.org) contains supplemental Tables S1 and S2.

[1] Supported by a United States Department of Defense postdoctoral award. Present address: University of Science and Technology, College of Life Science and Technology, Wuhan, Hubei 430074, China.

[2] Supported by National Institutes of Health Grants 5P30CA006516-43 and 1P01CA120964-01A1.

[3] To whom correspondence should be addressed: Dept. of Medicine, Beth Israel Deaconess Medical Center, 330 Brookline Ave., Boston, MA 02215. Tel.: 617-735-2065; Fax: 617-735-2050; E-mail: sbalk@bidmc.harvard.edu.

[4] The abbreviations used are: PI3K, phosphoinositide 3-kinase; RTK, receptor tyrosine kinase; PTEN, phosphate and tensin homolog; PCa, prostate cancer(s); GBM, glioblastoma multiforme; EGF, epidermal growth factor; siRNA, small interfering RNA; FBS, fetal bovine serum; LC, liquid chromatography; MS/MS, tandem mass spectrometry; TIC, total ion current; pAkt, phospho-Akt; Ab, antibody; EGFR, epidermal growth factor receptor; ERK, extracellular signal-regulated kinase; GPCR, G protein-coupled receptor; SH2, Src homology 2.

mutations in p110α can clearly contribute to tumorigenesis, recent studies suggest that PTEN-deficient cancers may be dependent on p110β, although this is not a consistent finding, and the molecular basis for this dependence is not known (17–21). A third mechanism that contributes to increased type IA PI3K signaling in tumors is overexpression or constitutive activation of certain RTKs. Indeed, PI3K activation by mutant EGFR in non-small cell lung cancer and by amplified ErbB2 in breast cancer are major mechanisms by which these RTKs drive tumor growth, and drugs that target these RTKs can suppress PI3K signaling and tumor growth (22, 23).

Therapeutic approaches to block PI3K in advanced PCa have focused on development of direct inhibitors of PI3K or its downstream effectors, in particular Akt. However, there has been little focus on blocking PI3K by targeting upstream RTKs because it has not been clear whether there is a requirement for p85 binding to activated RTKs or adaptor proteins in PTEN-deficient PCa cells. Significantly, a recent study in PTEN-deficient glioblastoma multiforme (GBM) showed that multiple RTKs were activated and required for p85 recruitment and PI3K activation and that PI3K activity could be abrogated through the simultaneous use of multiple RTK inhibitors (24). In this study, we examined whether particular RTKs are functioning as upstream activators of PI3K in PTEN-deficient PCa cells and are thereby potential therapeutic targets. The results demonstrate that basal PI3K activity in these cells is RTK-independent and mediated by p110β and p110δ, whereas PI3K activation in response to RTK stimulation is mediated by p110α.

EXPERIMENTAL PROCEDURES

Antibodies, Reagents, and Cells—Rabbit anti-pPRAS40 (Thr^{246}), anti-PI3K p85-conjugated agarose beads, mouse anti-Tyr(P) (4G10), and 4G10-conjugated agarose beads were from Upstate Biotechnology (Lake Placid, NY). Unconjugated rabbit anti-PI3K p85 polyclonal antibody was kindly provided by Dr. L. Cantley (Beth Israel Deaconess Medical Center, Boston, MA). Mouse anti-ErbB3 (2B5) was from Lab Vision (Fremont, CA). Rabbit polyclonal antibodies against EGF receptor (EGFR), ErbB2/Her2, Akt, pAkt (Ser^{473}), pAkt (Thr^{308}), ERK1/2, phospho-ERK1/2 (Thr^{202}/Tyr^{204}), Ras, and p85 binding motif (p*YXXM*) were from Cell Signaling (Danvers, MA). Mouse anti-PI3K p110α was from BD Biosciences (San Diego, CA). Rabbit anti-PI3K p110β and p110δ were from Abcam (Cambridge, MA) and Santa Cruz Biotechnology, Inc. (Santa Cruz, CA), respectively. Mouse anti-β-tubulin was from Chemicon (Temecula, CA). Rabbit IgG was from Vector Laboratories (Burlingame, CA). Normal mouse serum, protein A, and protein G beads were purchased from Pierce. Horseradish peroxidase-conjugated mouse and rabbit IgG were from Promega (Madison, WI).

PI3K inhibitor LY294002 was from Sigma. Ras inhibitor FTI-277 and Src inhibitor PP2 were obtained from Calbiochem, and another Src inhibitor, dasatinib, was kindly provided by Dr. N. Gray (Dana-Farber Cancer Institute, Boston, MA). Recombinant human heregulin-β1 and EGF were from R & D Systems (Minneapolis, MN). Protease inhibitor mixture tablets (EDTA-free) were from Roche Applied Science. ErbB3 siRNA and control siRNAs were from Dharmacon RNA Technologies (Lafayette, CO). The PTEN-deficient LNCaP, C4-2, and PC3 human prostate cancer cell lines were from ATCC and maintained in RPMI 1640 with 10% fetal bovine serum (FBS).

Immunoprecipitation and Immunoblotting—For anti-p85 immunoprecipitations, LNCaP or C4-2 cells grown in 10-cm plates were serum-starved for 3 days. They were then washed twice with cold 50 mM Tris-HCl buffer (pH 7.5) containing 150 mM NaCl (TBS) and lysed with TBS containing 1% Triton X-100, 1 mM Na_3VO_4, and a mixture of protease inhibitors. Cell lysates were sonicated for 10 s and centrifuged at 13,000 rpm, 4 °C for 15 min to remove cell debris. Cell lysates were precleared with rabbit IgG (preconjugated to protein A beads) at 4 °C for 45 min with continuous agitation. Cell lysates (1 mg) were mixed with 5 μg of p85 antibody in a final volume of 1 ml and incubated at 4 °C for 2 h with continuous agitation (5 μg of rabbit IgG was used as control). At the end of incubation, 20 μl of protein A beads were added, and samples were incubated at 4 °C for another 2 h with continuous agitation. The samples were then transferred to MicroSpin columns (Amersham Biosciences) with the bottoms deplugged. The beads were washed 6 times (600 μl each) in lysis buffer, followed by twice in TBS. The columns were spun at 1000 rpm for 30 s to remove extra buffer, and the column bottoms were then plugged. The immune complexes were eluted with 10 μl of Laemmli buffer without β-mecaptoethanol at 65 °C for 15 min and spun down at 2,000 rpm for 30 s. The flow-through was mixed with 1 μl of β-mecaptoethanol and boiled for 5 min. Proteins were resolved on 4–12% NuPAGE gels (Invitrogen), followed by membrane transfer and immunoblotting. Briefly, the membranes were blocked with 5% milk in TBS containing 0.2% Tween 20 (TBS/T) at room temperature for 2 h and incubated with primary antibodies at 4 °C overnight. After being washed with TBS/T, the membranes were incubated with appropriate horseradish peroxidase-conjugated secondary antibodies at room temperature for 1 h, washed, and developed with enhanced chemiluminescence reagents (PerkinElmer Life Sciences).

Immunoprecipitations with p85 antibody-conjugated agarose beads were carried out similarly. Briefly, 2 mg of cell lysates were mixed with 20 μl of p85 antibody conjugated agarose beads and incubated at 4 °C with continuous agitation overnight. Bead washing, elution, and immunoblotting were performed as described above. Immunoprecipitation with 4G10-conjugated beads was also performed as described above, except that serum-starved LNCaP or PC3 cells were lysed in radioimmune precipitation buffer (50 mM Tris-HCl, pH 8.0 containing 150 mM NaCl, 1% Nonidet P-40, 0.5% deoxycholate, 0.1% SDS) with 1 mM EDTA, 1 mM EGTA, 1 mM β-glycerophosphate, 1 mM pyrophosphate, 100 mM sodium fluoride, 1 mM Na_3VO_4, and a mixture of protease inhibitors.

For sequential immunoprecipitations with ErbB3 and p85 antibodies, LNCaP cells were lysed with TBS containing 1% Triton X-100 and a mixture of protease inhibitors. Cell lysates (1 mg) were immunoprecipitated with 5 μg of mouse anti-ErbB3 antibody or normal mouse serum and 20 μl of protein G beads. The beads were spun down at 1,000 rpm for 3 min and washed as described above. The supernatants were mixed with p85 antibody-conjugated agarose beads, and the immunopre-

cipitation was carried out as above. To analyze whether the interaction between p85 and RTKs was mediated by the SH2 domain of p85 recognizing pY*XX*M, LNCaP cells grown in 10-cm plates were serum-starved for 2 days and then treated with EGF (20 ng/ml, 5 min) or HRG-β1 (40 ng/ml, 15 min). Cells were then lysed and subjected to immunoprecipitation with anti-p85 or anti-Tyr(P), followed by blotting with the anti-pY*XX*M motif antibody.

LC/MS/MS Analysis—LNCaP and PC3 cells on 15-cm plates (20–40 plates) were lysed and subjected to immunoprecipitation with anti-p85, followed by mass spectrometry to identify p85-interacting proteins. Specifically, immunoprecipitates were resolved on 4–12% NuPAGE gels, followed by Coomassie Blue staining. Each lane was cut into multiple fragments, reduced with DTT, alkylated with iodoacetamide, and digested overnight with trypsin at pH 8.3. Tryptic peptides were extracted and then analyzed by data-dependent reversed-phase microcapillary tandem mass spectrometry (LC/MS/MS) using an LTQ two-dimensional linear ion trap mass spectrometer (Thermo Scientific, San Jose, CA) operated in positive ion mode at a flow rate of 250 nl/min. A 75 μm (inner diameter) $\times$ 15 μm (inner diameter tip) PicoFrit microcapillary column (New Objective, Woburn, MA) was self-packed with 5-μm C_{18} resin to 15 cm (length). The column was equilibrated, and peptides were loaded using buffer A (0.1% formic acid, 0.9% acetonitrile, 99% water) and then eluted with a gradient from 5% buffer B (acetonitrile) to 38% B, followed by 95% B for washing. One mass spectrometry survey scan was followed by eight MS/MS scans.

The Sequest algorithm in Proteomics browser software (Thermo Scientific, San Jose, CA) was used for data base searching of all MS/MS spectra against the reversed and concatenated Swiss-Prot protein data base with differential modifications: oxidation (+16 Da) of Met. Peptide sequences were initially accepted if they matched the forward data base and passed the following Sequest browser scoring thresholds: 2+ ions, Xcorr $\geq$ 2.0, Sf $\geq$ 0.4, $p \geq 0$; 3+ ions, Xcorr $\geq$ 2.65, Sf $\geq$ 0.5, $p \geq 5$. Peptides with gas phase charges of 1+ and 4+ were generally not accepted as valid due to difficulty of interpretation of such ions. After passing the scoring thresholds, all MS/MS were then manually inspected rigorously to be sure that all b− (fragment ions resulting from amide bond breaks from the peptide's N terminus) and y− ions (fragment ions resulting from amide bond breaks from the peptide's C terminus) aligned with the assigned protein data base sequence. Some digested samples were reanalyzed using an Orbitrap XL mass spectrometer (Thermo Scientific, San Jose, CA) in an attempt to discover additional proteins using a targeted ion MS/MS (TIMM) approach to search for known p85-binding proteins.[5] False discovery rates for peptide identifications were calculated to be less than 1.5%.

Quantification of PI3K Subunits—Relative quantification of the regulatory and catalytic subunits of PI3K in LNCaP and PC3 cells was achieved by utilizing a previously published method whereby the average total ion current (TIC) from MS/MS spectra for all peptides identifying each protein subunit was calculated and compared across all subunits (25). The method of quantifying different proteins within a single sample is valid because multiple peptides of varying ionization properties are averaged together, overcoming variability in peptide ionization efficiency. The calculations were processed using in-house developed software called *NakedQuant* version 1.0 (26). Supplemental Tables S1 and S2 list the peptides and TIC values used in the quantitative analysis.

siRNA Transfections—LNCaP cells (5×10^4/well) were seeded into 24-well plates 2 days before ErbB3 siRNA transfection, and 20 pmol of siRNAs in 2 μl of Lipofectamine were then added to each well. Media were replaced 24 h later, and cells were maintained in RPMI 1640 supplemented with 10% FBS for 24 h, followed by serum starvation for 48 h. Cells were then lysed with 100 μl of radioimmune precipitation buffer containing 1 mM Na_3VO_4 and a mixture of protease inhibitors. Cell lysates were centrifuged at 13,000 rpm, 4 °C for 15 min to remove cell debris, and 10 μg of total protein from each sample were resolved on 4–12% NuPAGE gels, followed by membrane transfer and immunoblotting. LNCaP cells grown in 10-cm plates were transfected with ErbB3 siRNA similarly to cells plated in 24-well plates, except that 120 pmol of siRNAs in 12 μl of Lipofectamine were used for each plate. After serum starvation for 48 h, cells were lysed with TBS containing 1% Triton X-100 and a mixture of protease inhibitors, followed by immunoprecipitation with p85 antibody and immunoblotting.

Drug Treatments—The dual EGFR/ErbB2 inhibitor lapatinib was used to investigate the effects of EGFR/ErbB2 on the phosphorylation of ErbB3. Serum-starved LNCaP cells grown in 10-cm plates were treated with lapatinib (10 μM) for 6 h. Cells were lysed and subjected to immunoprecipitation with anti-p85 or anti-Tyr(P) antibodies, followed by immunoblotting. To study the effects of Ras, serum-starved LNCaP and PC3 cells plated in 24-well plates were treated with farnesylation inhibitor FTI-277 (20 μM) for 2 days followed by EGF stimulation (20 ng/ml, 5 min). Cells were then lysed with TBS containing 1% Triton X-100 and a mixture of protease inhibitors followed by immunoblotting. To analyze whether phosphorylation of the catalytic p110 subunits was dependent on Src, LNCaP or PC3 cells grown on 10-cm plates were serum-starved for 1–2 days and then treated with either PP2 (10 μM, 2 h) or dasatinib (10 μM, 2 h). Afterward, cells were lysed and immunoprecipitated as above with p85 or 4G10 antibodies and immunoblotted. All experiments were performed at least three times, and representative gels are shown.

RESULTS

p85 Associates with Tyrosine-phosphorylated Proteins in Serum-starved PTEN-deficient PCa Cells—PI3K activity in PTEN intact cells is stimulated by binding of a p85 regulatory subunit SH2 domain to a tyrosine-phosphorylated RTK or adaptor protein, but the extent to which PI3K signaling is dependent on this p85-mediated activation step in PTEN-deficient PCa cells has not been determined. Significantly, each of the available PTEN-deficient PCa cell lines, LNCaP, C4-2 (derived from LNCaP), and PC3, has high levels of basal PI3K pathway activity (as assessed by immunoblotting for pAkt

[5] J. Asara, manuscript in preparation.

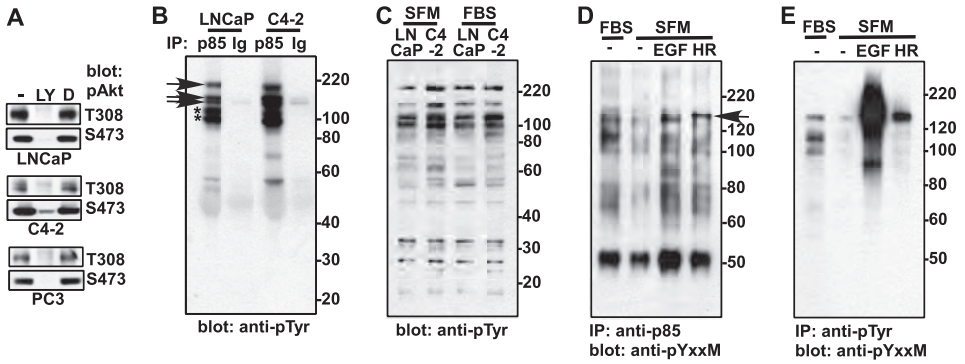

FIGURE 1. **p85 association with tyrosine-phosphorylated proteins in serum-starved PTEN-deficient PCa cells.** *A*, PTEN-deficient LNCaP, C4-2, or PC3 cells were cultured for 1–3 days in serum-free medium and then treated for 6 h with PI3K inhibitor LY294002 (*LY*; 20 μM) or vehicle control (DMSO) (*D*) or left untreated (−). Lysates (10 μg) were then immunoblotted for pAkt (Thr^{308} and Ser^{473}). *B*, serum-starved LNCaP or C4-2 cells (2–3 days) were lysed in TBS plus 1% Triton X-100, immunoprecipitated (*IP*) with anti-p85 or control rabbit Ig, and then immunoblotted with anti-Tyr(P) antibody (4G10). *C*, cell lysates (10 μg) from LNCaP or C4-2 cells grown in serum-free medium (*SFM*) or medium with 10% FBS were immunoblotted with anti-Tyr(P). *D* and *E*, LNCaP cells were either maintained in medium with 10% FBS or serum-starved for 2 days. Serum-starved cells were then stimulated with EGF (20 ng/ml, 5 min) or HRG-β1 (40 ng/ml, 15 min). Cell lysates were immunoprecipitated with anti-p85 (*D*) or anti-Tyr(P) (*E*), and the immunoprecipitates were blotted with anti-p*YXX*M. Molecular markers are indicated at the *margins*.

(Thr^{308} and Ser^{473}) even when cultured in serum-free medium for 2–3 days (Fig. 1*A*). Nonetheless, PI3K inhibition with LY294002 results in rapid loss of Akt phosphorylation, indicating that continuous PI3K activity is required to maintain downstream signaling even in the absence of PTEN.

To address whether this basal PI3K activity is dependent on p85 binding to one or a discrete subset of constitutively activated RTKs or adaptor proteins, we initially determined whether p85 was associated with tyrosine-phosphorylated proteins in serum-starved LNCaP or C4-2 cells. Cells were serum-starved for 3 days, lysates were immunoprecipitated with anti-p85 antibody, and the precipitated proteins were then immunoblotted with an anti-Tyr(P) antibody. This analysis in LNCaP cells revealed two major lower bands that were consistent with the p85 regulatory and p110 catalytic subunits of PI3K (*asterisks*) and three more slowly migrating bands of ~190, 150, and 130 kDa (*arrows*) (Fig. 1*B*). An identical pattern was observed in C4-2 cells (Fig. 1*B*). These bands were specific because they were not precipitated by a control rabbit Ig, and they represented only a subset of the total input cellular tyrosine-phosphorylated proteins (Fig. 1*C*).

The p85 subunit SH2 domains associate with tyrosine-phosphorylated proteins through binding to p*YXX*M motifs in RTKs and adaptor proteins (2). To determine whether constitutive tyrosine phosphorylation of a specific protein was mediating p85 recruitment directly through SH2 domain binding, we next immunoblotted the p85 immunoprecipitates with a p*YXX*M motif-specific antibody. Discrete major p85-associated bands at ~190 kDa were detected by the anti-p*YXX*M antibody after EGF or heregulin-β1 stimulation, with the band after heregulin-β1 (arrow) being consistent with ErbB3 (which contains six p*YXX*M motifs) (Fig. 1*D*). The antibody detected several proteins in the p85 immunoprecipitates from LNCaP cells grown in 10% FBS. A series of weaker bands were observed in cells cultured in serum-free medium, but they did not clearly correspond to the discrete bands between 130 and 190 kDa detected by the anti-Tyr(P) Ab.

As a further sensitive assay to detect proteins containing p*YXX*M motifs in serum-starved LNCaP cells, whole cell lysates were immunoprecipitated with an anti-Tyr(P) Ab and then immunoblotted with the p*YXX*M motif Ab. As shown in Fig. 1*E*, several bands could be detected when cells were grown in 10% FBS, but these were markedly diminished in the serum-starved cells. As expected, stimulation with EGF or heregulin-β1 resulted in a dramatic increase in a band consistent with ErbB3. Taken together, these data suggested that the association between p85 and tyrosine-phosphorylated proteins (detected in Fig. 1*B*) was not due to direct p85 SH2 domain-mediating binding.

p85-associated Proteins Identified by LC/MS/MS—Although major specific p85-associated proteins in serum-starved LNCaP cells were not detected by the p*YXX*M motif antibody, the interactions that were weakly detected by this antibody or more readily detected by the Tyr(P) antibody (see Fig. 1*B*) may nonetheless be physiologically significant in PTEN-deficient cells. Therefore, we next focused on the identification of p85-associated proteins using liquid chromatography/tandem mass spectrometry (LC/MS/MS). Anti-p85 beads were used to carry out large scale immunopurifications from serum-starved LNCaP cells, which were then run on SDS-PAGE. Multiple gel slices corresponding to protein molecular masses from ~60 to 220 kDa were then subjected to in-gel trypsin digestion, and eluted peptides were identified by LC/MS/MS (Table 1) using a linear ion trap mass spectrometer. As expected, a large fraction of the peptides detected in the ~100 kDa range were from the α and β isoforms of p85 and the p110 PI3K catalytic subunits. Interestingly, peptide recovery indicated that p110β and p110δ were the major p85-associated p110 isoforms, with much lower levels of p110α (see below).

Among the p85-associated proteins identified initially by LC/MS/MS, only ErbB3 had been shown previously to mediate p85 SH2 domain binding and PI3K activation (Table 1). To further assess whether there was an interaction between ErbB3 and p85 in serum-starved cells, we carried out immunoblotting of p85 immunoprecipitates with anti-ErbB3, which confirmed the interaction in LNCaP and C4-2 cells (Fig. 2*A*). On a subsequent LC/MS/MS analysis of the p85 immunoprecipitates using a more sensitive Orbitrap XL mass spectrometer, we also detected GAB1 (Table 1). However, we could not detect GAB1 associated with p85 by immunoblotting (data not shown). Consistent with the LC/MS/MS data, we similarly did not find detectable levels of ErbB2, EGFR, c-MET, insulin-like growth factor receptor, insulin receptor, IRS-2, or IRS-4 (LNCaP cells are IRS-1-deficient) in the p85 immunoprecipitates by immunoblotting (data not shown).

TABLE 1
p85-associated proteins identified by LC/MS/MS in LNCaP cells

Accession	Protein name	Spectral count
PIK3R2	Phosphatidylinositol 3-kinase regulatory subunit β	34
PK3CB	Phosphatidylinositol-4,5-bisphosphate 3-kinase catalytic subunit β isoform	25
PK3CD	Phosphatidylinositol-4,5-bisphosphate 3-kinase catalytic subunit δ isoform	24
PIK3R1	Phosphatidylinositol 3-kinase regulatory subunit α	17
MAP1B	Microtubule-associated protein 1B	12
EWS	RNA-binding protein EWS	10
FAS	Fatty acid synthase	8
MYH10	Myosin-10	8
LIMC1	LIM and calponin homology domain-containing protein 1	6
RFIP1	Rab11 family-interacting protein 1	6
MYH9	Myosin-9	5
MYO6	Myosin-VI	5
PK3CA	Phosphatidylinositol 4,5-bisphosphate 3-kinase catalytic subunit α isoform	5
TERA	Transitional endoplasmic reticulum ATPase	5
SYEP	Bifunctional aminoacyl-tRNA synthetase	4
IF4G1	Eukaryotic translation initiation factor 4 γ 1	4
ILF3	Interleukin enhancer-binding factor 3	4
PNPT1	Polyribonucleotide nucleotidyltransferase 1, mitochondrial	4
SFPQ	Splicing factor, proline- and glutamine-rich	4
SMRC1	SWI/SNF complex subunit SMARCC1	4
DHX9	ATP-dependent RNA helicase A	3
RAD50	DNA repair protein RAD50	3
MATR3	Matrin-3	3
TPR	Nucleoprotein TPR	3
K1967	Deleted in breast cancer gene 1 protein (DBC.1) (DBC-1) (p30 DBC)	3
TFR1	Transferrin receptor protein 1	3
SC16A	Protein transport protein Sec16A	2
ERBB3	Receptor tyrosine protein kinase ErbB-3	2
GAB1[a]	GRB2-associated binding protein 1	2
NUCL	Nucleolin	1

[a] Identified in a subsequent analysis focused on targeting peptides from known p85-interacting proteins.

p85 Interaction with ErbB3 Is Independent of ErbB3 Phosphorylation and ErbB2 Activity—The ErbB3 polypeptide is 148 kDa, but it is glycosylated and migrates at ~185 kDa on SDS-PAGE, which suggested that the p85-associated tyrosine phosphorylated band at ~190 kDa might be ErbB3. To test this hypothesis, we determined whether depleting ErbB3 by immunoprecipitation with anti-ErbB3 would decrease the p85-associated ~190 kDa tyrosine-phosphorylated band in a subsequent anti-p85 immunoprecipitation. As shown in Fig. 2*B* (*top left*), ErbB3 could be substantially depleted from a LNCaP whole cell lysate by an initial immunoprecipitation with anti-ErbB3. The ErbB3 depletion also markedly decreased the amount of ErbB3 that was coprecipitated with p85 (Fig. 2*B*, *bottom left*). However, this ErbB3 depletion did not decrease the intensity of the tyrosine-phosphorylated band at ~190 kDa or other bands that were coprecipitated by anti-p85. Moreover, an anti-Tyr(P) blot of ErbB3 immunoprecipitated by the anti-ErbB3 Ab showed that ErbB3 was not substantially tyrosine-phosphorylated (Fig. 2*B*, *right panels*).

This result indicated that ErbB3 was not one of the major tyrosine-phosphorylated proteins associated with p85. However, we could not rule out the possibility that a small pool of heavily tyrosine-phosphorylated ErbB3 was associated with p85 and was not efficiently immunoprecipitated by the anti-ErbB3. Therefore, we next used siRNA to down-regulate ErbB3 expression. As shown in Fig. 2*C*, total ErbB3 expression was markedly reduced by ErbB3 siRNA *versus* a control siRNA. ErbB3 associated with p85 was also decreased, although this decrease was less marked than the decrease in total ErbB3, suggesting a relatively high affinity p85-ErbB3 interaction. Importantly, there was again no clear decrease in the p85-associated tyrosine-phosphorylated protein at ~190 kDa (Fig. 2*D*). Moreover, there was no evident effect of the ErbB3 siRNA on PI3K activity, as assessed by Akt phosphorylation at Ser^{473} or Thr^{308} (Fig. 2*C*). Taken together, these results demonstrated that p85 was constitutively associated with ErbB3 in LNCaP cells, but this interaction appeared to be independent of ErbB3 phosphorylation and was not clearly required for PI3K activity.

To further address whether ErbB3 phosphorylation made any contribution to the p85-ErbB3 interaction or PI3K activity, we treated LNCaP cells with a dual EGFR/ErbB2 inhibitor (lapatinib) to further suppress any basal tyrosine phosphorylation of ErbB3 mediated by EGFR or ErbB2. Using an anti-Tyr(P) immunoprecipitation, followed by immunoblotting to detect tyrosine phosphorylated proteins, we found that lapatinib (10 μM for 6 h) suppressed the basal tyrosine phosphorylation of both EGFR and ErbB2 in serum-starved LNCaP cells (Fig. 3*A*). Consistent with the results in Figs. 1 and 2, there was no readily detectable ErbB3 in the anti-Tyr(P) immunoprecipitation. Moreover, there was no detectable effect of lapatinib on PI3K activity, as assessed by Akt phosphorylation (Fig. 3*A*). Significantly, lapatinib did not decrease the interaction between p85 and ErbB3, further supporting the conclusion that this interaction is independent of ErbB3 phosphorylation by ErbB2 or EGFR (Fig. 3*B*). Surprisingly, the intensity of the p85-associated band at ~190 kDa detected by Tyr(P) immunoblotting was selectively decreased by lapatinib, suggesting that it may be an EGFR or ErbB2 substrate that is binding directly or indirectly to p85 (Fig. 3*C*). In any case, although the identity of this ~190-kDa protein remains to be determined, it does not appear to contribute to PI3K activity.

p85 Is Not Associated with Tyrosine-phosphorylated Proteins in PC3 Cells—To further assess the possible importance of p85 membrane recruitment by tyrosine-phosphorylated proteins,

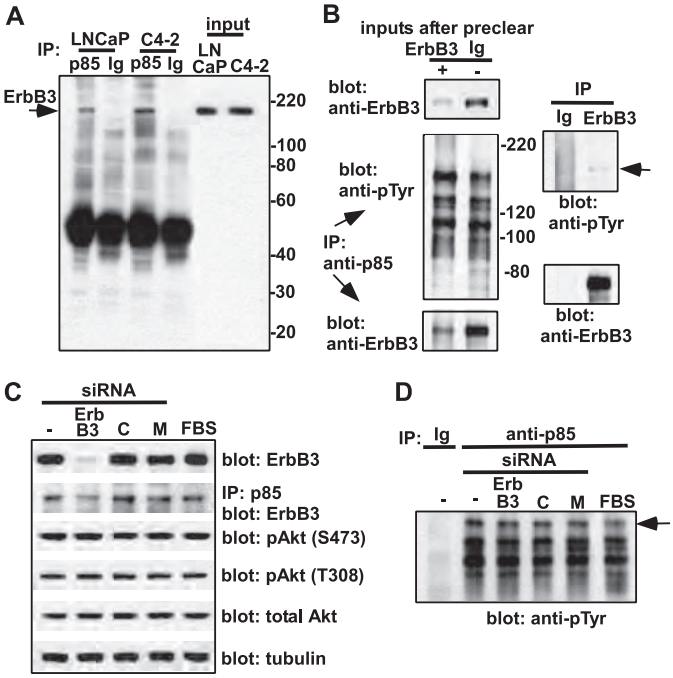

FIGURE 2. **p85 interacts with ErbB3 independently of ErbB3 phosphorylation.** *A*, lysates from serum-starved LNCaP or C4-2 cells (2 days) were immunoprecipitated (*IP*) with anti-p85 (p85) or control rabbit IgG (*Ig*), followed by blotting for ErbB3. Input is 1% of the material used for coimmunoprecipitation. *B*, LNCaP cells maintained in medium with 10% FBS were lysed in TBS plus 1% Triton X-100 and immunoprecipitated with anti-ErbB3 or control Ig, followed by anti-p85. The p85 immunoprecipitates were immunoblotted with anti-Tyr(P) (*middle left*) or anti-ErbB3 (*bottom left*). *Top left*, level of ErbB3 remaining in the anti-ErbB3 or Ig precleared lysates before the p85 immunoprecipitation. *Right panels*, anti-Tyr(P) (*top*) or anti-ErbB3 blots of initial anti-ErbB3 or Ig control immunoprecipitates. The *arrow* indicates a faint band at ~190 kDa consistent with ErbB3. *C* and *D*, LNCaP cells transfected with ErbB3 or control non-targeted siRNA (*C*), or mock-transfected (*M*), were maintained in 10% FBS medium for 24 h, followed by serum starvation for 48 h. A portion of each cell lysate (10 μg) was then immunoblotted as indicated (*C*). The remaining lysates were immunoprecipitated with anti-p85, followed by immunoblotting with anti-ErbB3 (*C*) or anti-Tyr(P) (*D*). Molecular markers are indicated at the *margins*. The *arrow* indicates the position of proteins around 190 kDa.

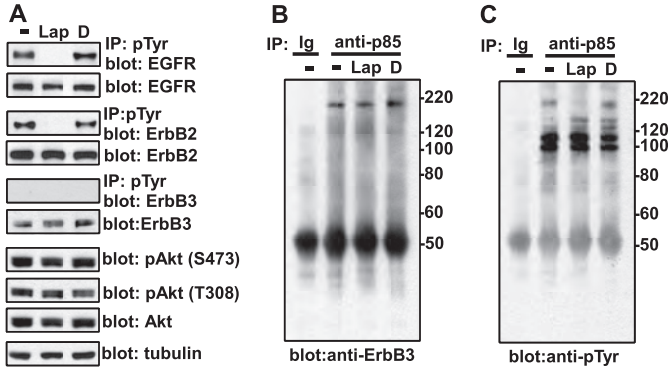

FIGURE 3. **PI3K activity and p85-ErbB3 interaction in LNCaP cells are independent of EGFR/ErbB2 activity.** Serum-starved LNCaP cells (2 days) on 10-cm plates were treated with EGFR/ErbB-2 dual inhibitor lapatinib (10 μM) or vehicle (DMSO; *D*) for 6 h. *A*, cell lysates were immunoprecipitated (*IP*) with anti-Tyr(P), followed by immunoblotting for EGFR, ErbB2, or ErbB3. Whole cell lysates prior to immunoprecipitation were also immunoblotted as indicated for input EGFR, ErbB2, ErbB3, and Akt and for pAkt. *B* and *C*, cell lysates were immunoprecipitated with anti-p85 or rabbit IgG (*Ig*), followed by immunoblotting for ErbB3 (*B*) or Tyr(P) (*C*).

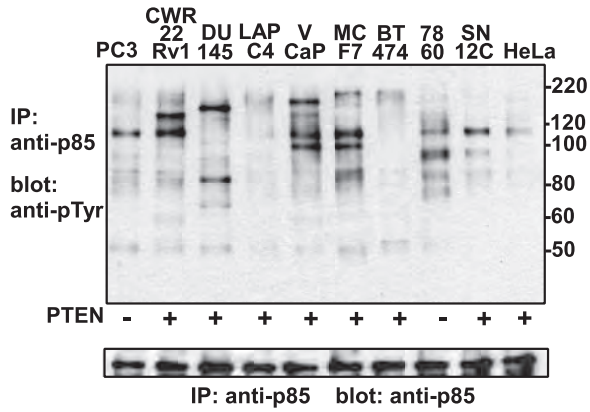

FIGURE 4. **p85 is not associated with tyrosine-phosphorylated proteins in PC3 cells.** Human PCa cell lines PC3, CWR22Rv1, DU145, LAPC4, and VCaP; human breast cancer lines MCF7 and BT474; human renal carcinoma cell lines 786O (PTEN deficient) and SN12C; and a human cervical cancer cell line (HeLa) grown in 10-cm plates were serum-starved for 1 day. Cell lysates were immunoprecipitated (*IP*) with anti-p85 and immunoblotted with anti-Tyr(P) (*top*) or anti-p85 (*bottom*). Molecular markers are indicated at the *right*.

we examined p85-associated tyrosine-phosphorylated proteins from PC3 cells (also a PTEN-deficient PCa cell line) and a series of other cell lines in serum-free medium. Significantly, the only major tyrosine-phosphorylated band associated with p85 in PC3 cells was ~110 kDa, consistent with the PI3K catalytic subunits (Fig. 4). It should be noted that anti-Tyr(P) binding to this ~110-kDa protein could possibly be nonspecific because the PI3K p110 catalytic subunit, which is tightly associated with p85, is the major protein on these blots. However, it appears to be specific because comparable amounts of p85 were immunoprecipitated from each of the other cell lines, but the ~110 kDa band was found to be tyrosine-phosphorylated in only a subset of the cells. Tyrosine phosphorylation of this band does not appear to correlate with PTEN status (CWR22, DU145, LAPC4, and VCaP are PCa cell lines with intact PTEN) or cell type. Interestingly, additional major p85-associated tyrosine-phosphorylated bands were detected in other cells, but their identities and significance with respect to PI3K activity remain to be determined. In any case, these results in PC3 cells support the conclusion that SH2 domain-mediated binding of p85 to a tyrosine-phosphorylated RTK or adaptor protein is not required for basal PI3K activity in PTEN-deficient PCa cells.

p110 Phosphorylation Is Mediated by c-Src and Is Not Required for PI3K Activity—Although the functional significance of PI3K p110 tyrosine phosphorylation is not clear, we next considered that it may be contributing to PI3K activity in PTEN-deficient PCa cells. To further assess whether the p85-associated tyrosine-phosphorylated proteins at ~110 kDa were PI3K catalytic subunits, we first carried out anti-Tyr(P) immunoprecipitations from serum-starved LNCaP and PC3 cells, followed by immunoblotting for each of the p110 isoforms. As shown in Fig. 5*A*, substantial levels of p110β and lower levels of p110δ were precipitated by the anti-Tyr(P) antibody in both cells, whereas there was no detectable p110α (not shown). It should be noted that p110 in these experiments could possibly be precipitated indirectly through an association with another tyrosine-phosphorylated protein, although the lack of other p85-associated tyrosine-phosphorylated proteins in PC3 cells suggests that it is being precipitated directly.

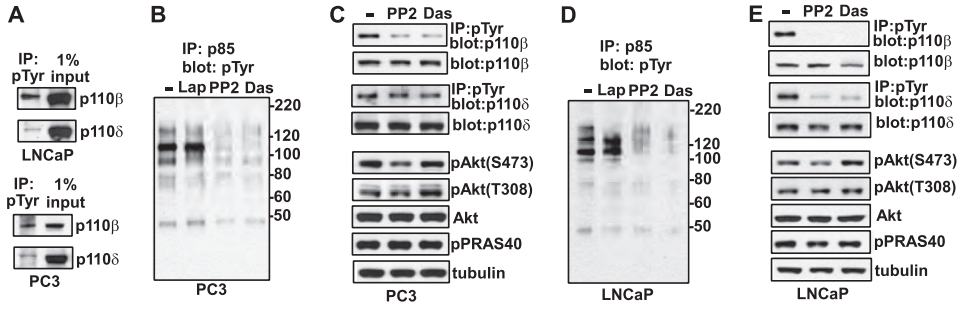

FIGURE 5. **p110 tyrosine phosphorylation is mediated by c-Src and is not required for PI3K activity.** *A*, serum-starved LNCaP (2 days) and PC3 cells (1 day) were lysed and immunoprecipitated (*IP*) with anti-Tyr(P), followed by immunoblotting for anti-p110β or -δ. Input is 1% of the material used for the precipitation. *B*, serum-starved PC3 cells (1 day) were treated with lapatinib or Src inhibitors PP2 or dasatinib for 2 h, all at 10 μM. Cell lysates (1 mg) were then immunoprecipitated with anti-p85 and immunoblotted with anti-Tyr(P). *C*, serum-starved PC3 cells (1 day) were treated with PP2 or dasatinib at 10 μM for 2 h. Cell lysates were then immunoprecipitated with anti-Tyr(P), followed by immunoblotting with anti-p110β or -δ. Whole cell lysates (10 μg) were immunoblotted with pAkt, pPRAS40, or total Akt. *D*, serum-starved LNCaP cells (2 days) were treated with lapatinib, PP2, or dasatinib for 2 h, all at 10 μM. Cell lysates (1 mg) were immunoprecipitated with anti-p85 and immunoblotted with anti-Tyr(P). *E*, serum-starved LNCaP cells (2 days) were treated with PP2 or dasatinib at 10 μM for 2 h. Cell lysates were immunoprecipitated with anti-Tyr(P), followed by blotting with anti-p110β or -δ. Whole cell lysates (10 μg) were immunoblotted with pAkt, pPRAS40, or total Akt. Molecular markers are indicated at the *right* in *B* and *D*.

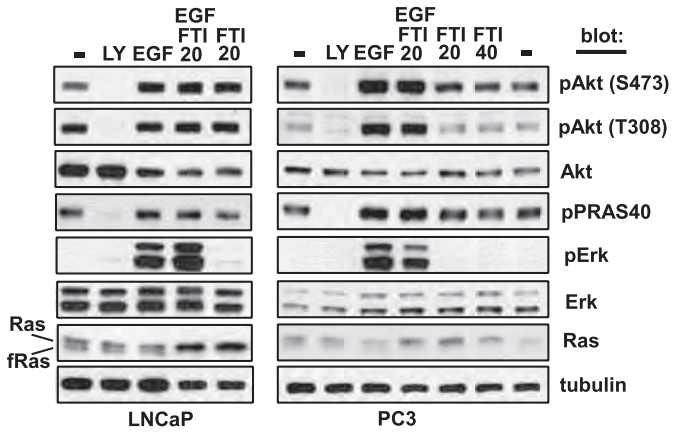

FIGURE 6. **PI3K pathway activity in PTEN-deficient PCa cells is Ras-independent.** LNCaP (*left*) or PC3 cells (*right*) plated into 24-well plates were treated with farnesylation inhibitor FTI-277 (20 or 40 μM; prepared in serum-free medium) for 2 days, and non-drug-treated wells were serum-starved for the same duration. At the end of FTI-277 treatment, cells were either treated with LY294002 (20 μM, 2 h) or stimulated with EGF (20 ng/ml, 5 min). Whole cell lysates (10 μg) were analyzed by immunoblotting for pAkt, pPRAS40, total Akt, ERK1/2, phospho-ERK1/2, Ras, or tubulin. *Upper* and *lower bands* corresponding to Ras and farnesylated Ras (*fRas*) are indicated.

Lapatinib treatment did not decrease the major ~110-kDa tyrosine-phosphorylated band that coprecipitates with p85 in PC3 cells, indicating that it was not phosphorylated by EGFR or ErbB2 (Fig. 5*B*). To identify other tyrosine kinases that may be mediating p110 phosphorylation, we used public data bases (Phosphosite and Scansite, available on the World Wide Web) to determine previously identified sites of tyrosine phosphorylation on the PI3K p110 catalytic subunits and candidate kinases for these sites, which suggested phosphorylation by c-Src or a c-Src family kinase. Strikingly, treatment with c-Src inhibitors (PP2 or dasatinib) resulted in the complete loss of the p85-associated tyrosine-phosphorylated band at 110 kDa in serum-starved PC3 cells (Fig. 5*B*). Consistent with p110β being the predominant tyrosine-phosphorylated p110 isoform in PC3 cells, Tyr(P) immunoprecipitation, followed by p110 blotting, showed a marked decline in p110β tyrosine phosphorylation (Fig. 5*C*). However, c-Src inhibition did not clearly suppress Akt phosphorylation or activity, as assessed by phosphorylation of the Akt substrate PRAS40 (Fig. 5*C*).

As shown in Fig. 3, lapatinib treatment of LNCaP cells resulted in loss of the p85-associated tyrosine-phosphorylated band at ~190 kDa but did not decrease the bands at ~110 or ~130–150 kDa (Fig. 5*D*). In contrast, PP2 and dasatinib markedly decreased all of the p85-associated tyrosine-phosphorylated bands in LNCaP cells. Consistent with the tyrosine-phosphorylated band at ~110 kDa in the LNCaP cells being PI3K catalytic subunits, PP2 and dasatinib markedly decreased p110β and p110δ tyrosine phosphorylation (Fig. 5*E*). However, as observed in PC3 cells, these c-Src inhibitors did not substantially decrease PI3K activity as assessed by Akt phosphorylation and activity (Fig. 5*E*). These results demonstrate that tyrosine phosphorylation of the PI3K catalytic subunit is mediated by c-Src (or a Src family kinase) but does not contribute to PI3K activity. Moreover, the results further support the conclusion that basal PI3K activity is not dependent on p85 recruitment by an activated RTK or adaptor protein.

PI3K Pathway Activity in PTEN-deficient PCa Cells Is Ras-independent—An alternative mechanism by which RTKs may recruit and activate PI3K is by generating GTP-Ras, which can bind to the p110 subunits via Ras binding domains located carboxyl to the p85 binding domains (27). GTP-Ras has been shown to enhance p110α activity, and an intact p110α-Ras interaction is required for Ras-mediated tumorigenesis, although the importance of GTP-Ras for other p110 isoforms has not been established (28, 29). The LC/MS/MS analysis of p85-associated proteins from LNCaP cells did not reveal an association of Ras, and this was confirmed by immunoblotting of anti-p85 immunoprecipitates with a pan-anti-Ras antibody (data not shown). However, a weak transient interaction could not be excluded. Therefore, to further assess whether Ras was contributing to PI3K pathway activation, we treated serum-starved LNCaP and PC3 cells with a farnesylation inhibitor, FTI-277. Immunoblotting with a pan-anti-Ras Ab confirmed that the drug prevented formation of the more rapidly migrating farnesylated protein (*fRas*), but there was no effect on PI3K pathway activation in serum-starved LNCaP or PC3 cells (Fig. 6). It should be noted that the drug did not abrogate EGF-mediated ERK activation, indicating either that adequate Ras could still be recruited (farnesylated or independent of farnesylation) or that EGFR was signaling independently of Ras.

Distinct p110 Isoforms Mediate Basal Versus Growth Factor-stimulated PI3K Activity—It was noteworthy that the LC/MS/MS analysis of p85 associated proteins in LNCaP cells indicated that p110β and p110δ were the major isoforms (Table

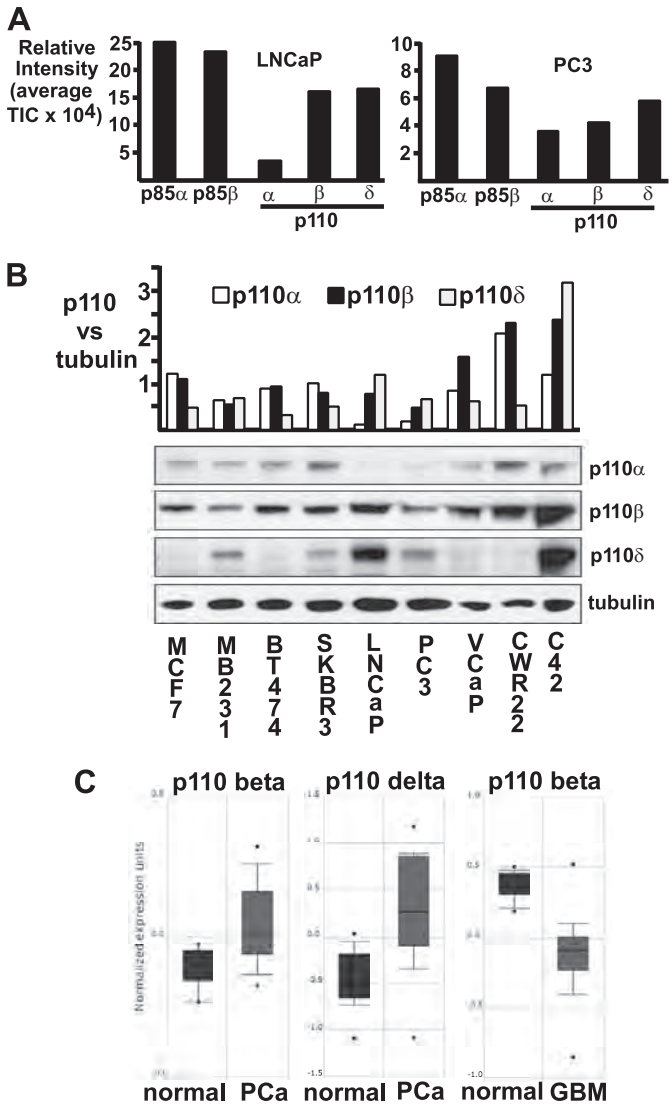

FIGURE 7. **Expression of PI3K p110 isoforms in PCa cell lines.** *A*, LC/MS/MS analyses of the relative abundance by average TIC of the PI3K subunits p85α and -β and p110α, -β, and -δ in LNCaP and PC3 cells. *B*, expression levels of p110 isoforms in a variety of cancer cell lines based on immunoblotting. 10 μg of cell lysates from breast cancer lines (MCF-7, MB-MDA-231, BT-474, and SKBR-3) or PCa cell lines (LNCaP, PC3, VCaP, CWR22Rv1, and C4-2) were analyzed by immunoblotting with p110 isoform-specific antibodies. Intensity of each band relative to tubulin is shown. *C*, p110β and p110δ mRNA levels in normal prostate *versus* PCa or normal brain *versus* GBM. Expression data were generated by Oncomine based on results from Vanaja *et al.* (30) (PCa p110β), Dhanasekaran *et al.* (31) (PCa p110δ), and Sun *et al.* (33) (GBM).

1). In addition, a label-free quantitative LC/MS/MS analysis based on the calculated average TIC (25) of all identified peptides corresponding to PI3K protein subunits was utilized to quantify the relative abundance of PI3K regulatory and catalytic subunits in both LNCaP and PC3 cell lines. This analysis for LNCaP was consistent with Table 1 and for PC3 cells also showed lower levels of p110α, although the levels in PC3 were closer to those of p110β and p110δ (Fig. 7*A*) (see supplemental Tables S1 and S2 for PI3K quantification). Results from immunoblotting LNCaP and PC3 whole cell lysates with isoform-specific p110 Abs were in general agreement with the LC/MS/MS data (Fig. 7*B*). Moreover, the immunoblotting indicated that p110α levels in LNCaP and PC3 cells were lower than in a small series of breast cancer lines and in PCa cells with intact PTEN (VCaP and CWR22) (Fig. 7*B*). Interestingly, available cDNA/oligonucleotide microarray data show that p110β and p110δ mRNA, but not p110α mRNA, are increased in PCa *versus* normal prostate (Fig. 7*C*) (data not shown) (30, 31). A recent immunohistochemical study similarly found an increase in p110β in PCa *versus* normal prostate epithelium (32). In contrast, microarray data in GBM, which is also characterized by PTEN loss, shows that p110β is decreased (Fig. 7*C*) (33).

Based on these observations, we addressed whether the basal PI3K activity in PC3 and LNCaP cells, which appears to be independent of p85 binding to RTKs or adaptor proteins, was mediated by a particular p110 isoform. Significantly, siRNA-mediated depletion of p110β, but not p110α or p110δ, decreased PI3K activity in serum-starved PC3 cells (Fig. 8*A*). This result is consistent with a recent study using p110β short hairpin RNA in PC3 cells, which showed that PI3K activity and tumor growth (*in vitro* and *in vivo*) were p110β-dependent (17). In contrast, PI3K pathway activation in PC3 cells in response to heregulin-β1 was suppressed by depletion of p110α but not p110β or p110δ (Fig. 8*B*). In serum-starved LNCaP cells, siRNA targeting both p110β and p110δ (which is expressed at higher levels in LNCaP *versus* PC3 cells) decreased PI3K activity, whereas p110α siRNA again had no effect (Fig. 8*C*). However, as in PC3 cells, only the p110α siRNA decreased PI3K pathway activation in response to heregulin-β1 (Fig. 8*D*). Finally, we addressed whether basal PI3K activity could be further suppressed by simultaneously silencing both p110β and -δ. As shown in Fig. 8, *E* and *F*, targeting both p110β and -δ did not appear to be more effective. We presume this reflects an inability to completely silence both p110β and -δ, but it remains possible that p110α can mediate some basal activity in the absence of other catalytic subunits. Taken together, these results indicate that basal PI3K activity in LNCaP and PC3 cells is mediated through p110β and p110δ (in LNCaP) and that this activity is independent of RTK-mediated p85 recruitment.

DISCUSSION

Activation of class IA PI3Ks by RTKs is mediated through binding of p85 regulatory subunit Src homology 2 domains, recognizing pY*XX*M motifs, to tyrosine-phosphorylated RTKs or adaptor proteins. PTEN loss enhances and prolongs the PI3K signal, but some level of basal PI3K activity is still required to maintain the activation of downstream targets, such as Akt. This study examined whether the high basal PI3K activity in PTEN-deficient PCa cells was dependent on p85 recruitment by one or a small subset of RTKs, which might then be therapeutic targets. Immunoblotting of p85-associated proteins in serum-starved PTEN-deficient LNCaP and C4-2 PCa cells showed a small set of discrete tyrosine-phosphorylated proteins, but these proteins were not clearly recognized by an anti-pY*XX*M motif antibody and were not observed in PTEN-deficient PC3 cells. LC/MS/MS analysis of proteins that coimmunoprecipitated with p85 showed that ErbB3 was associated with p85 in serum-starved LNCaP cells, but this interaction was independent of ErbB3 tyrosine phosphorylation and was not required for basal PI3K activity. Using siRNA specific for each

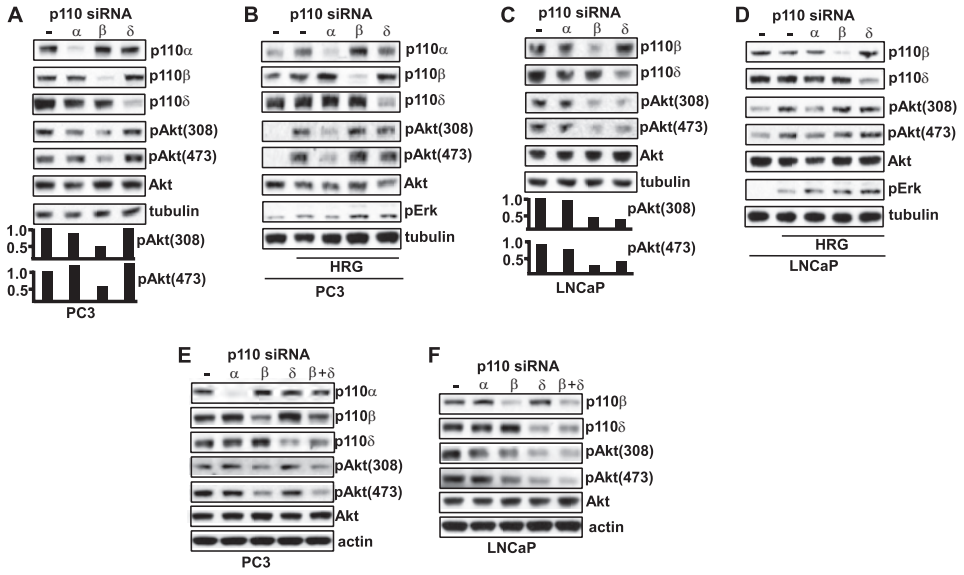

FIGURE 8. **Distinct p110 isoforms mediate basal *versus* growth factor-stimulated PI3K activity.** PC3 (*A*) or LNCaP (*C*) cells in 24-well plates were transfected with siRNAs for each p110 isoform. After serum starvation for 1–2 days, cells were lysed, and 10 μg of cell lysates were subjected to immunoblotting for each p110 isoform, pAkt, total Akt, or β-tubulin. Results are quantified in *bar graphs* and are representative of 2–3 independent experiments for each cell type (in addition to results in *E* and *F*). PC3 (*B*) or LNCaP (*D*) transfected with siRNAs for each p110 isoform were serum-starved for 1–2 days, followed by HRG-β1 stimulation (100 ng/ml, 15 min). Cell lysates were then subjected to immunoblotting as indicated. *E* and *F*, PC3 or LNCaP cells, respectively, were transfected with siRNAs for each p110 isoform or with both p110β and -δ siRNA and were then analyzed by immunoblotting after serum starvation for 2 days.

p110 isoform, we found that this basal PI3K activity was mediated by p110β in PC3 cells and by both p110β and p110δ in LNCaP cells, whereas p110α was required for PI3K activation in response to RTK stimulation by heregulin-β1. Taken together, these findings indicate that basal PI3K activity in PTEN-deficient PCa cells is RTK-independent and mediated by p110β and p110δ.

The p110β dependence of basal PI3K activity is consistent with a recent study using inducible short hairpin RNA targeting p110α or p110β, which similarly found that PI3K activity in PC3 cells, as well as PTEN-deficient U87MG glioma cells and BT549 breast cancer cells, was dependent on p110β (17). This recent study also showed that p110β depletion decreased PI3K activity and growth *in vivo* in PC3 xenografts. The *in vivo* importance of p110β for PI3K activation and growth in PTEN-deficient PCa is further supported by a study showing that loss of p110β but not p110α could decrease Akt activation and development of neoplasia in the anterior prostate of mice with prostate-specific PTEN deletion (although this previous study did not examine the ventral and dorsolateral prostate, which are more closely related to human prostate) (18).

Our finding that PI3K activation in response to heregulin-β1 is dependent on p110α extends previous results showing that p110α is the major isoform activated in response to some other RTKs, such as insulin receptor in liver, although this is not a consistent finding and may be cell type-dependent (18, 21, 34–38). However, the molecular basis for this preferential coupling of RTKs to p110α is not clear, and the extent to which additional RTKs in other cell types are coupled selectively to p110α remains to be determined.

The mechanisms mediating basal p110β and p110δ activation in serum-starved LNCaP cells and p110β activation in PC3 cells are similarly unclear. In contrast to p110α, previous studies indicate that p110β may be activated through binding to G protein-coupled receptors (GPCRs) (38–41). In preliminary studies, we have not observed an effect of pertussis toxin on basal PI3K activity, but this toxin only blocks a subset of GPCRs. Alternatively, p110β may have a modest level of constitutive activity in the absence of RTK or GPCR stimulation that is adequate to maintain PI3K pathway activation in PTEN-deficient cells. In support of this hypothesis, p110β overexpression has been found to mediate the transformation of fibroblasts (42).

In contrast to our findings in PTEN-deficient PCa, a recent study that focused on PTEN-deficient GBM cells found that p85 was associated with multiple activated RTKs and adaptor proteins under serum-starved conditions and that combination therapies targeting multiple RTKs could suppress PI3K activity in PTEN-intact and -deficient tumor cells (24). The RTK dependence for basal PI3K activity suggests that PTEN-deficient GBM cells lack RTK-independent mechanisms for activation of p110β or p110δ or possibly express p110β at too low a level for any constitutive activity to sustain PI3K pathway activation. This apparent biological difference between PTEN-deficient PCa and GBM cell lines may reflect an abundance of peptide growth factors in the microenvironment during GBM development or the absence of pathways mediating RTK-independent p110β or p110δ activation. A biological difference between PTEN-deficient PCa and GBM with respect to PI3K signaling is further supported by gene expression studies, which indicate that p110α is increased relative to p110β in GBM, whereas p110β is increased in PCa (see Fig. 7). However, the extent to which RTKs in GBM are signaling through p110α *versus* other isoforms remains to be determined.

It is noteworthy that PI3K pathway activation in PCa is frequently due to PTEN loss, with activating mutations in p110α that are found in other cancers being rare in PCa. The reason for this preference is not clear, but it is presumed to reflect nonredundant functions of other PI3K catalytic subunits that are required for prostate carcinogenesis and possibly additional PTEN-regulated pathways distinct from PI3K. In any case, the findings in this study suggest that prostate epithelial cells that have sustained genetic or epigenetic loss of PTEN activity may be dependent initially on p110β (or possibly p110δ) for PI3K pathway activation and positive selection due to a relative lack of growth factors mediating activation of RTKs and p110α in the microenvironment of the fully developed adult human prostate. If this hypothesis is correct, then selective p110β inhibitors or inhibitors of particular GPCRs or other upstream

activators of p110β, if present, may be most effective at early stages of PCa development. In contrast, because disease progression is probably associated with increased RTK stimulation and activation of p110α, the extent to which selective inhibition of p110β will be effective in more advanced PCa is not clear and may be dependent on whether it still has a nonredundant downstream function.

REFERENCES

1. Engelman, J. A., Luo, J., and Cantley, L. C. (2006) *Nat. Rev. Genet.* **7,** 606–619
2. Songyang, Z., Shoelson, S. E., Chaudhuri, M., Gish, G., Pawson, T., Haser, W. G., King, F., Roberts, T., Ratnofsky, S., and Lechleider, R. J. (1993) *Cell* **72,** 767–778
3. Yu, J., Zhang, Y., McIlroy, J., Rordorf-Nikolic, T., Orr, G. A., and Backer, J. M. (1998) *Mol. Cell. Biol.* **18,** 1379–1387
4. Carracedo, A., and Pandolfi, P. P. (2008) *Oncogene* **27,** 5527–5541
5. Keniry, M., and Parsons, R. (2008) *Oncogene* **27,** 5477–5485
6. Yuan, T. L., and Cantley, L. C. (2008) *Oncogene* **27,** 5497–5510
7. Zhao, L., and Vogt, P. K. (2008) *Oncogene* **27,** 5486–5496
8. Cairns, P., Okami, K., Halachmi, S., Halachmi, N., Esteller, M., Herman, J. G., Jen, J., Isaacs, W. B., Bova, G. S., and Sidransky, D. (1997) *Cancer Res.* **57,** 4997–5000
9. McMenamin, M. E., Soung, P., Perera, S., Kaplan, I., Loda, M., and Sellers, W. R. (1999) *Cancer Res.* **59,** 4291–4296
10. Wang, S. I., Parsons, R., and Ittmann, M. (1998) *Clin. Cancer Res.* **4,** 811–815
11. Rubin, M. A., Gerstein, A., Reid, K., Bostwick, D. G., Cheng, L., Parsons, R., and Papadopoulos, N. (2000) *Hum. Pathol.* **31,** 504–508
12. Feilotter, H. E., Nagai, M. A., Boag, A. H., Eng, C., and Mulligan, L. M. (1998) *Oncogene* **16,** 1743–1748
13. Wang, S., Gao, J., Lei, Q., Rozengurt, N., Pritchard, C., Jiao, J., Thomas, G. V., Li, G., Roy-Burman, P., Nelson, P. S., Liu, X., and Wu, H. (2003) *Cancer Cell* **4,** 209–221
14. Trotman, L. C., Niki, M., Dotan, Z. A., Koutcher, J. A., Di Cristofano, A., Xiao, A., Khoo, A. S., Roy-Burman, P., Greenberg, N. M., Van Dyke, T., Cordon-Cardo, C., and Pandolfi, P. P. (2003) *PLoS Biol.* **1,** E59
15. Backman, S. A., Ghazarian, D., So, K., Sanchez, O., Wagner, K. U., Hennighausen, L., Suzuki, A., Tsao, M. S., Chapman, W. B., Stambolic, V., and Mak, T. W. (2004) *Proc. Natl. Acad. Sci. U.S.A.* **101,** 1725–1730
16. Samuels, Y., Wang, Z., Bardelli, A., Silliman, N., Ptak, J., Szabo, S., Yan, H., Gazdar, A., Powell, S. M., Riggins, G. J., Willson, J. K., Markowitz, S., Kinzler, K. W., Vogelstein, B., and Velculescu, V. E. (2004) *Science* **304,** 554
17. Wee, S., Wiederschain, D., Maira, S. M., Loo, A., Miller, C., deBeaumont, R., Stegmeier, F., Yao, Y. M., and Lengauer, C. (2008) *Proc. Natl. Acad. Sci. U.S.A.* **105,** 13057–13062
18. Jia, S., Liu, Z., Zhang, S., Liu, P., Zhang, L., Lee, S. H., Zhang, J., Signoretti, S., Loda, M., Roberts, T. M., and Zhao, J. J. (2008) *Nature* **454,** 776–779
19. Torbett, N. E., Luna-Moran, A., Knight, Z. A., Houk, A., Moasser, M., Weiss, W., Shokat, K. M., and Stokoe, D. (2008) *Biochem. J.* **415,** 97–110
20. Oda, K., Okada, J., Timmerman, L., Rodriguez-Viciana, P., Stokoe, D., Shoji, K., Taketani, Y., Kuramoto, H., Knight, Z. A., Shokat, K. M., and McCormick, F. (2008) *Cancer Res.* **68,** 8127–8136
21. Jia, S., Roberts, T. M., and Zhao, J. J. (2009) *Curr. Opin. Cell Biol.* **21,** 199–208
22. Engelman, J. A., and Cantley, L. C. (2006) *Clin. Cancer Res.* **12,** 4372s–4376s
23. Engelman, J. A., Jänne, P. A., Mermel, C., Pearlberg, J., Mukohara, T., Fleet, C., Cichowski, K., Johnson, B. E., and Cantley, L. C. (2005) *Proc. Natl. Acad. Sci. U.S.A.* **102,** 3788–3793
24. Stommel, J. M., Kimmelman, A. C., Ying, H., Nabioullin, R., Ponugoti, A. H., Wiedemeyer, R., Stegh, A. H., Bradner, J. E., Ligon, K. L., Brennan, C., Chin, L., and DePinho, R. A. (2007) *Science* **318,** 287–290
25. Asara, J. M., Christofk, H. R., Freimark, L. M., and Cantley, L. C. (2008) *Proteomics* **8,** 994–999
26. Yang, X., Friedman, A., Nagpal, S., Perrimon, N., and Asara, J. M. (2009) *J. Biomol. Tech.* **20,** 272–277
27. Pacold, M. E., Suire, S., Perisic, O., Lara-Gonzalez, S., Davis, C. T., Walker, E. H., Hawkins, P. T., Stephens, L., Eccleston, J. F., and Williams, R. L. (2000) *Cell* **103,** 931–943
28. Gupta, S., Ramjaun, A. R., Haiko, P., Wang, Y., Warne, P. H., Nicke, B., Nye, E., Stamp, G., Alitalo, K., and Downward, J. (2007) *Cell* **129,** 957–968
29. Rodriguez-Viciana, P., Sabatier, C., and McCormick, F. (2004) *Mol. Cell. Biol.* **24,** 4943–4954
30. Vanaja, D. K., Cheville, J. C., Iturria, S. J., and Young, C. Y. (2003) *Cancer Res.* **63,** 3877–3882
31. Dhanasekaran, S. M., Dash, A., Yu, J., Maine, I. P., Laxman, B., Tomlins, S. A., Creighton, C. J., Menon, A., Rubin, M. A., and Chinnaiyan, A. M. (2005) *FASEB J.* **19,** 243–245
32. Zhu, Q., Youn, H., Tang, J., Tawfik, O., Dennis, K., Terranova, P. F., Du, J., Raynal, P., Thrasher, J. B., and Li, B. (2008) *Oncogene* **27,** 4569–4579
33. Sun, L., Hui, A. M., Su, Q., Vortmeyer, A., Kotliarov, Y., Pastorino, S., Passaniti, A., Menon, J., Walling, J., Bailey, R., Rosenblum, M., Mikkelsen, T., and Fine, H. A. (2006) *Cancer Cell* **9,** 287–300
34. Chaussade, C., Rewcastle, G. W., Kendall, J. D., Denny, W. A., Cho, K., Grønning, L. M., Chong, M. L., Anagnostou, S. H., Jackson, S. P., Daniele, N., and Shepherd, P. R. (2007) *Biochem. J.* **404,** 449–458
35. Foukas, L. C., Claret, M., Pearce, W., Okkenhaug, K., Meek, S., Peskett, E., Sancho, S., Smith, A. J., Withers, D. J., and Vanhaesebroeck, B. (2006) *Nature* **441,** 366–370
36. Knight, Z. A., Gonzalez, B., Feldman, M. E., Zunder, E. R., Goldenberg, D. D., Williams, O., Loewith, R., Stokoe, D., Balla, A., Toth, B., Balla, T., Weiss, W. A., Williams, R. L., and Shokat, K. M. (2006) *Cell* **125,** 733–747
37. Zhao, J. J., Cheng, H., Jia, S., Wang, L., Gjoerup, O. V., Mikami, A., and Roberts, T. M. (2006) *Proc. Natl. Acad. Sci. U.S.A.* **103,** 16296–16300
38. Guillermet-Guibert, J., Bjorklof, K., Salpekar, A., Gonella, C., Ramadani, F., Bilancio, A., Meek, S., Smith, A. J., Okkenhaug, K., and Vanhaesebroeck, B. (2008) *Proc. Natl. Acad. Sci. U.S.A.* **105,** 8292–8297
39. Ciraolo, E., Iezzi, M., Marone, R., Marengo, S., Curcio, C., Costa, C., Azzolino, O., Gonella, C., Rubinetto, C., Wu, H., Dastrù, W., Martin, E. L., Silengo, L., Altruda, F., Turco, E., Lanzetti, L., Musiani, P., Rückle, T., Rommel, C., Backer, J. M., Forni, G., Wymann, M. P., and Hirsch, E. (2008) *Sci. Signal.* **1,** ra3
40. Murga, C., Fukuhara, S., and Gutkind, J. S. (2000) *J. Biol. Chem.* **275,** 12069–12073
41. Hazeki, O., Okada, T., Kurosu, H., Takasuga, S., Suzuki, T., and Katada, T. (1998) *Life Sci.* **62,** 1555–1559
42. Kang, S., Denley, A., Vanhaesebroeck, B., and Vogt, P. K. (2006) *Proc. Natl. Acad. Sci. U.S.A.* **103,** 1289–1294